Supporting information

Turn-On Fluorescent Sensors for the Selective Detection of Al^{3+}(and Ga^{3+}) and PPi Ions

Vijay Kumar,[⊥] Pramod Kumar,[⊥] Sushil Kumar,[⊥] Divya Singhal and Rajeev Gupta*

Department of Chemistry, University of Delhi, New Delhi 110007, India

EXPERIMENTAL SECTION

Physical Measurements. Elemental analysis data were obtained by Elementar Analysen Systeme GmbH Vario EL-III instrument. ^{1}H and ^{13}C NMR spectra were recorded with a JEOL 400 MHz instrument. FTIR spectra (Zn–Se ATR) were recorded with a Perkin-Elmer Spectrum-Two spectrometer. The absorption spectra were recorded with a Perkin-Elmer Lambda–25 spectrophotometer. Fluorescence spectral studies were performed with a Cary Eclipse fluorescence spectrophotometer. High-resolution mass spectra were obtained with Agilent Q-TOF LC-MS mass spectrometer. Time-resolved fluorescence spectra were recorded with a picosecond spectrofluorimeter from Horiba Jobin Yvon (FluoroHub).

Determination of Binding Parameters. Detection limits were calculated[1,2] using equation (1), where σ is the standard deviation of ten blank emission measurements of chemosensors **L1-L4** and k is the slope of a plot "difference in intensities (I-I0)" against "concentration of guest [Al^{3+} or Ga^{3+}]". The binding constants (K_b) were determined from the ratio of intercept and slope of the straight line of Benesi-Hildebrand plot of $1/(I\text{-}I_0)$ against $1/[M^{3+}]$ (M^{3+} = Al^{3+} or Ga^{3+}) (equation 2);[2,3] where I_0 and I are the fluorescence intensities of chemosensors **L1-L4** in absence and presence of M^{3+} ion, respectively and I_{min} is the minimum emission intensity in presence of M^{3+} ion.

$$\text{Detection limit} = 3\sigma/k \qquad (1)$$

$$1/(I\text{-}I_0) = 1/\{K_b(I_0 - I_{min})[M^{3+}]\} + 1/(I_0 - I_{min}) \qquad (2)$$

^{1}H NMR Spectral Titrations. ^{1}H NMR spectra of chemosensor **L4** (2 mM) was recorded in DMSO-d^6 in the absence as well as in the presence of $Al(NO_3)_3 \cdot 9H_2O$ (2-10 equivalents).

X-ray Crystallography. The intensity data for **L1** was collected with an Oxford XCalibur CCD diffractometer equipped with graphite monochromatic Mo-Kα radiation (λ = 0.71073 Å)[4]. Data reduction was performed with CrysAllisPro program (Oxford Diffraction ver. 171.34.40).[4] The structure was solved by direct methods using SIR-92 program[5] and refined on F2 using all data by full matrix least-squares procedures with SHELXL-2014/7.[6] The hydrogen atoms were placed at the calculated positions and included in last cycles of the refinement. All calculations were done using the WinGX software package.[7] The crystallographic data collection and structure solution parameters are summarized in Table S1 (Supporting Information).

Electrochemistry. The cyclic voltammetric experiments were performed using a CH Instruments electrochemical analyzer (Model 1120A). The cell contained a glassy-carbon electrode, a Pt wire auxiliary electrode, and Ag^{+}/Ag as the reference electrode.[8] The solutions were ca. 1 mM in complex and ca. 0.1 M in supporting electrolyte, TBAP.[8]

Low Cost Detection. For colorimetric analysis[9,10] standard solutions of investigated metal ions (2 equivalents) were added to the ethanolic solution of chemosensor **L4** and photographs were taken under the visible light. For detection by paper strips,[9,10] Whatman filter paper strips were immersed in a solution of chemosensor **L4** in ethanol and were air-dried to prepare the paper test strips. Such test strips coated with **L4** were dipped for a few seconds directly into a solution of each metal ion. Such paper test strips were then investigated under the visible light.

Fabrication of Polystyrene Films. A mixture of styrene (0.5 mL), α,α'-azoisobutyronitrile (AIBN, 1 mg) and chemosensor **L4** in CH_3OH (0.5 mL) was heated on water bath at 80 ºC for 30 min. Subsequently, a few drops of the aforementioned hot clear solution were poured over a glass-slide and the resultant glass-slide was air-dried to produce a thin film of polystyrene.[9] Such

polymeric films were peelable from the glass slide; however, glass-slides containing polymeric film were used for the detection Al^{3+} and Ga^{3+} ions by directing dipping into the aqueous solution (containing 5% EtOH) of $Al(NO_3)_3 \cdot 9H_2O$ and $GaCl_3$. Such glass-slides containing polystyrene films were then photographed under the visible and ultraviolet light.

References

1. (a) Kumar, P.; Kumar, V.; Gupta, R. Arene-based fluorescent probes for the selective detection of iron. *RSC Adv.* **2015**, *5*, 97874-97882. (b) Kumar, P.; Kumar, V.; Gupta, R. Selective fluorescent turn-off sensing of Pd^{2+} ion: applications as paper strips, polystyrene films, and in cell imaging. *RSC Adv.* **2017**, *7*, 7734-7741.
2. (a) Pandey, S.; Kumar, P.; Gupta, R. Polymerization led selective detection and removal of Zn^{2+} and Cd^{2+} ions: isolation of Zn- and Cd-MOFs and reversibility studies. *Dalton Trans.* **2018**, *47*, 14686-14695. (b) Kumar, S.; Kishan, R.; Kumar, P.; Pachisia, S.; Gupta, R. Size-Selective Detection of Picric Acid by Fluorescent Palladium Macrocycles. *Inorg. Chem.* **2018**, 57, 1693-1697.
3. Benesi, H. A.; Hildebrand, J. H. A Spectrophotometric Investigation of the Interaction of Iodine with Aromatic Hydrocarbons. *J. Am. Chem. Soc.* **1949**, 71, 2703-2707.
4. CrysAlisPro, v. 1.171.33.49b, Oxford Diffraction Ltd., **2009**.
5. Altomare, A.; Cascarano, G.; Giacovazzo, C.; Guagliardi, A. Completion and refinement of crystal structures with SIR92. *J. Appl. Crystallogr.* **1993**, *26*, 343-350.
6. (a) Sheldrick, G. M. *SHELXL-2014/7*: *Program for the solution of crystal structures*, University of Gottingen, Gottingen, Germany, **2014**. (b) Sheldrick, G. M.; A short history of SHELX *Acta Crystallogr. Sect. A: Found Crystallogr.* **2008**, *64*, 112-122.

7. Farrugia, L. J. WinGX, v. 1.70, *An Integrated System of Windows Programs for the Solution, Refinement and Analysis of Single- Crystal X-ray Diffraction Data*, Department of Chemistry, University of Glasgow, **2003**.
8. (a) Sawyer, D. T.; Roberts, J. L. *Experimental Electrochemistry for Chemists*, Wiley, New York, 1974; (b) Connelly, N. G.; Geiger, W. E. *Chem. Rev*., **1996**, *96,* 877-910.
9. Kumar, P.; Kumar, V.; Gupta, R. Selective fluorescent turn-off sensing of Pd^{2+} ion: applications as paper strips, polystyrene films, and in cell imaging. *RSC Adv.* **2017**, *7*, 7734-7741.
10. Wang, M.; Liu, X.; Lu, H.; Wang, H.; Qin, Z. Highly selective and reversible chemosensor for Pd(2+) detected by fluorescence, colorimetry, and test paper. *ACS Appl. Mater. Interfaces* **2015**, *7*, 1284-1289.

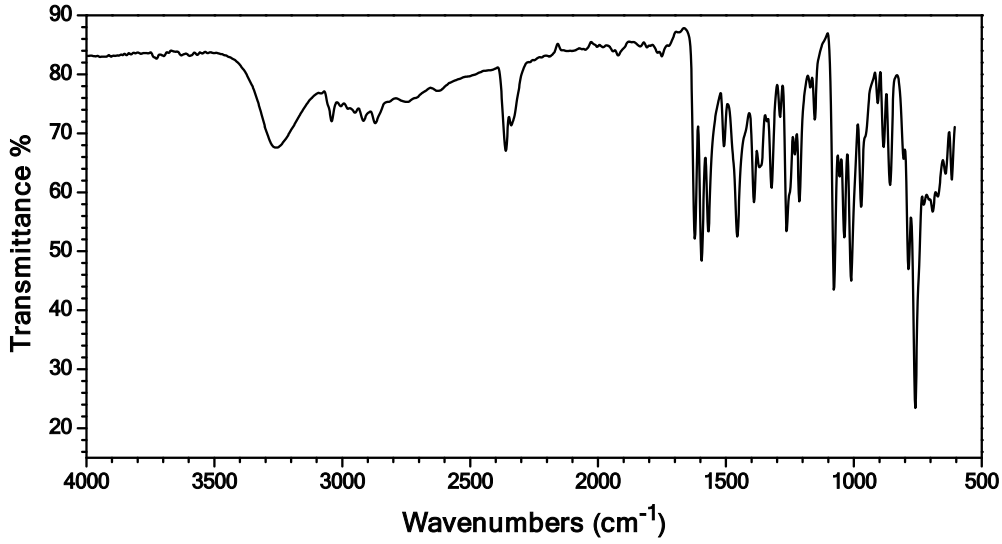

Figure S1. FTIR spectrum of chemosensor **L1**.

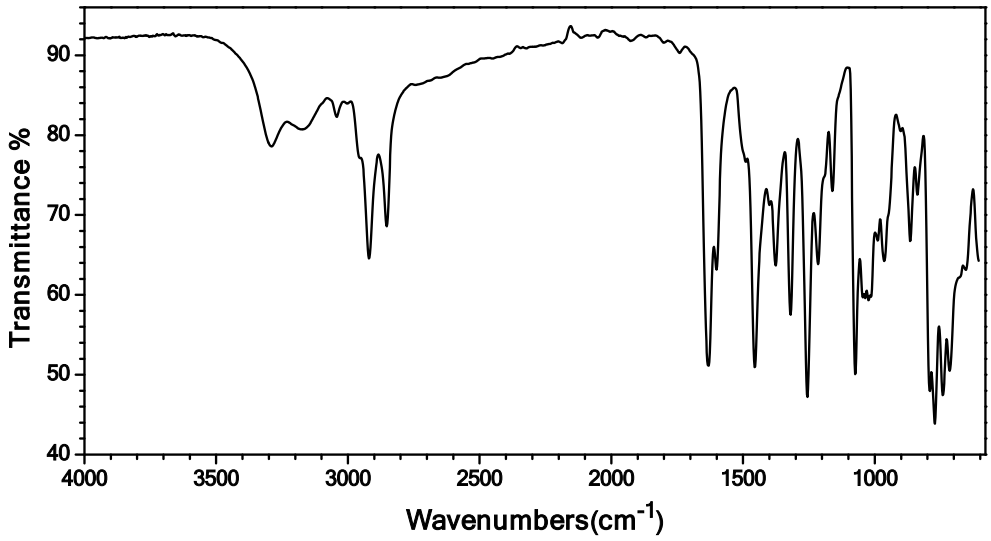

Figure S2. FTIR spectrum of chemosensor **L2**.

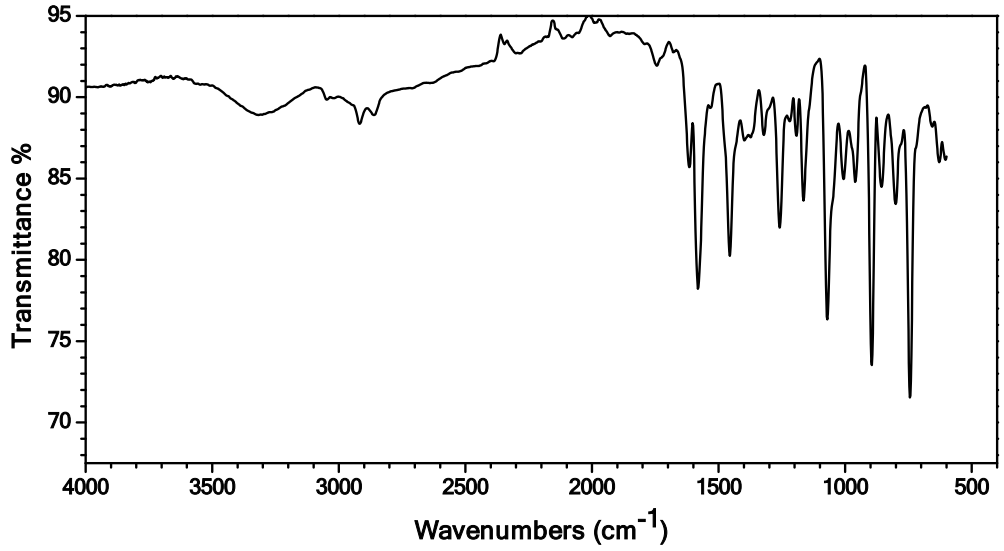

Figure S3. FTIR spectrum of chemosensor **L3**.

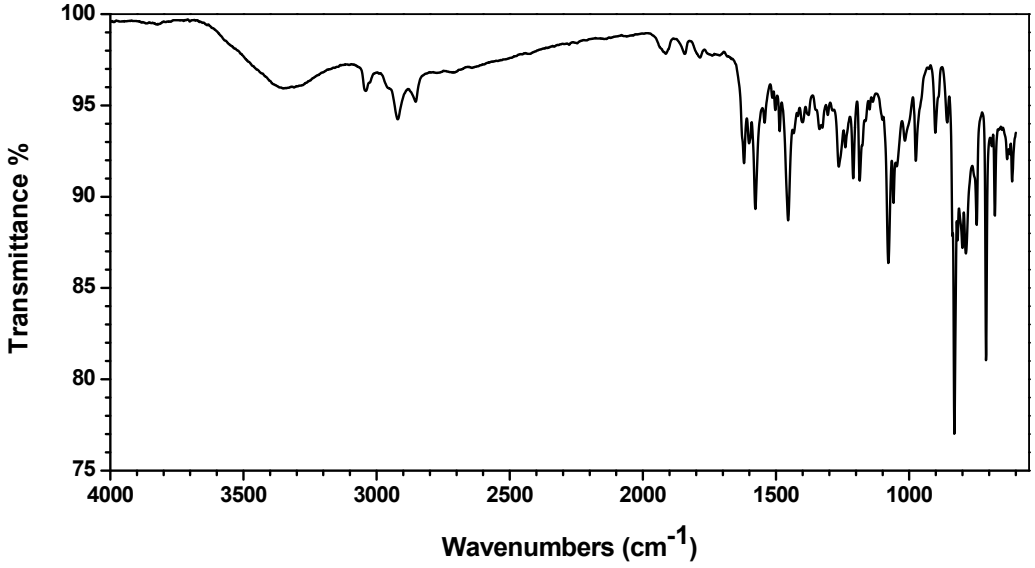

Figure S4. FTIR spectrum of chemosensor **L4**.

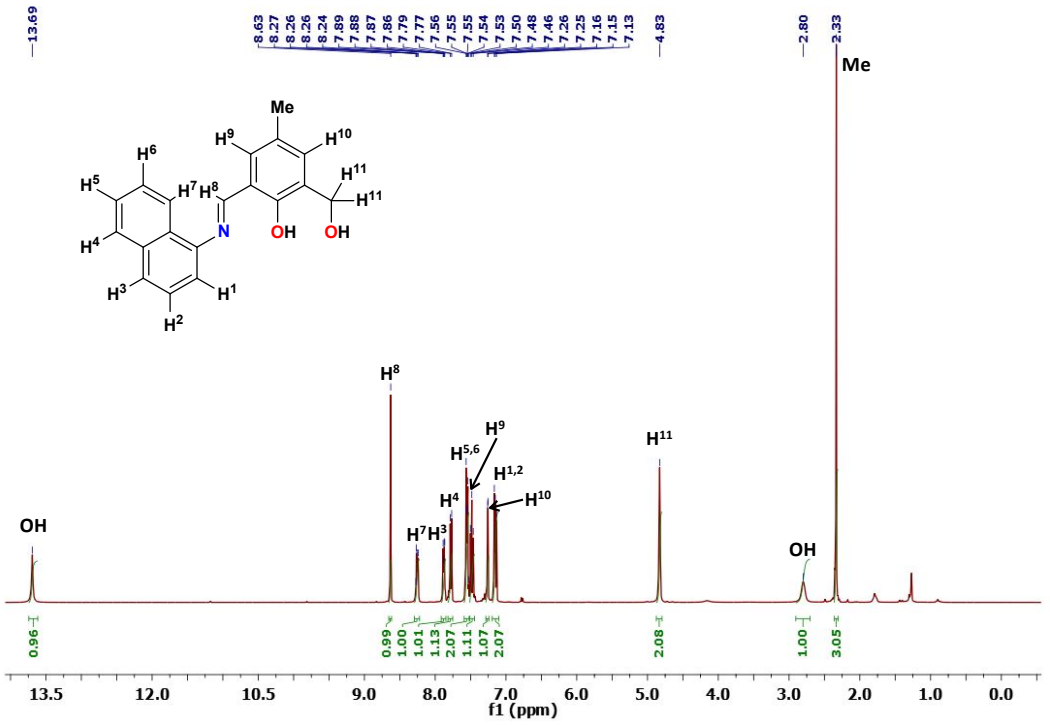

Figure S5. ^{1}H NMR spectrum of chemosensor **L1** in $CDCl_3$.

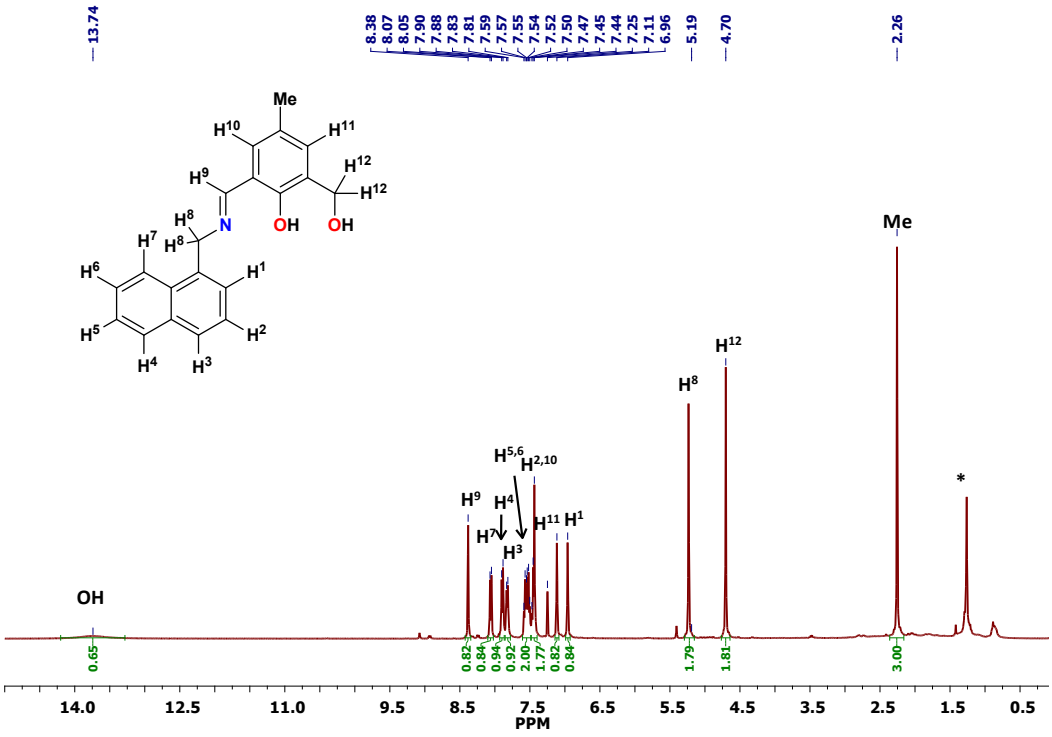

Figure S6. ^{1}H NMR spectrum of chemosensor **L2** in $CDCl_3$.

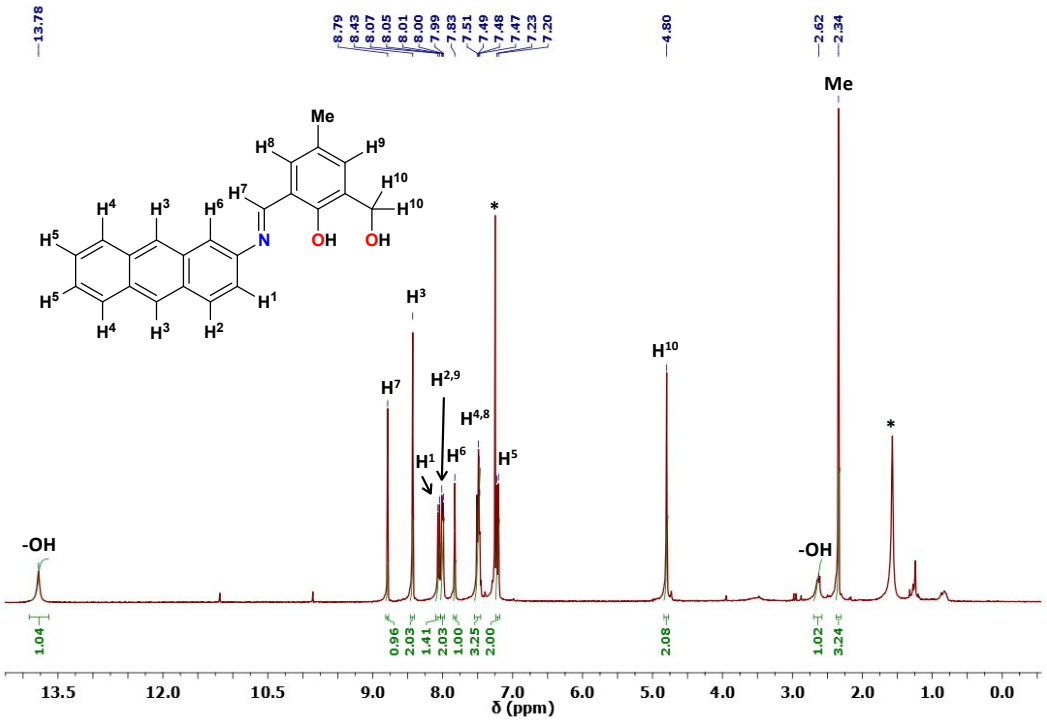

Figure S7. ^{1}H NMR spectrum of chemosensor **L3** in $CDCl_3$.

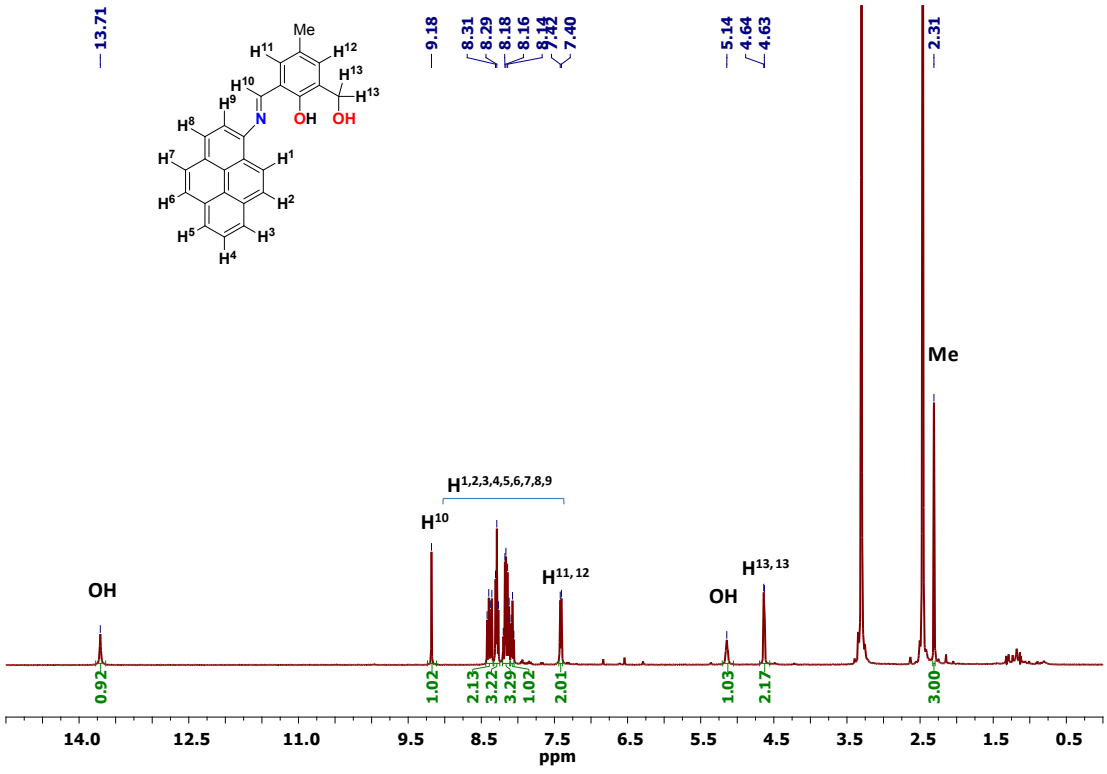

Figure S8. ^{1}H NMR spectrum of chemosensor **L4** in DMSO-d6.

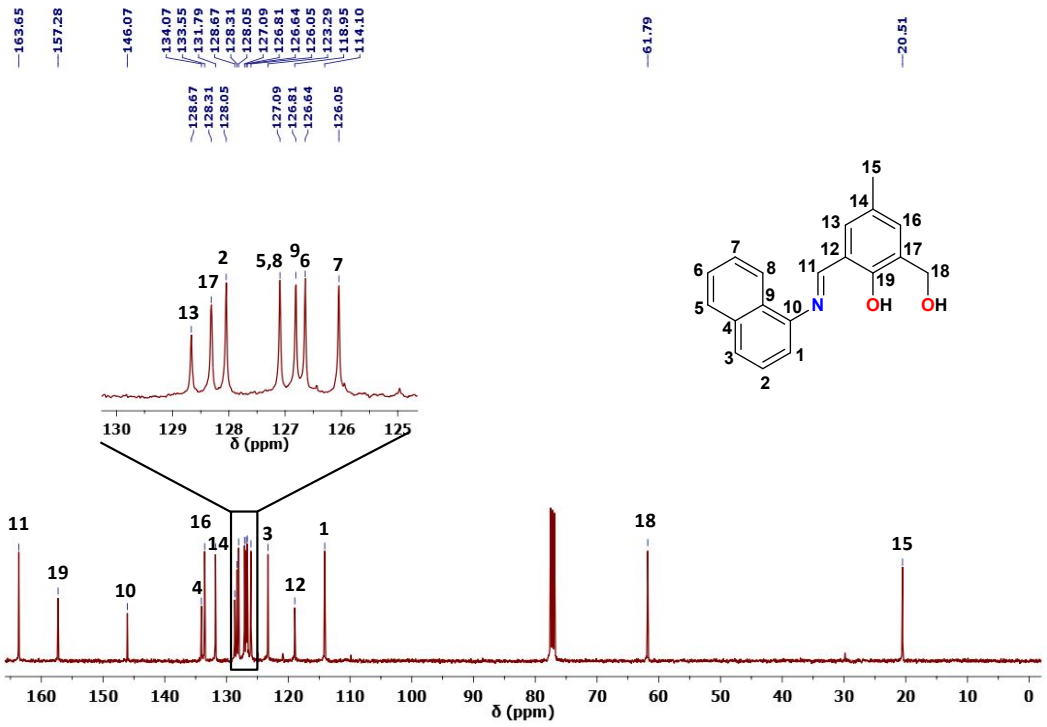

Figure S9. ^{13}C NMR spectrum of chemosensor **L1** in $CDCl_3$.

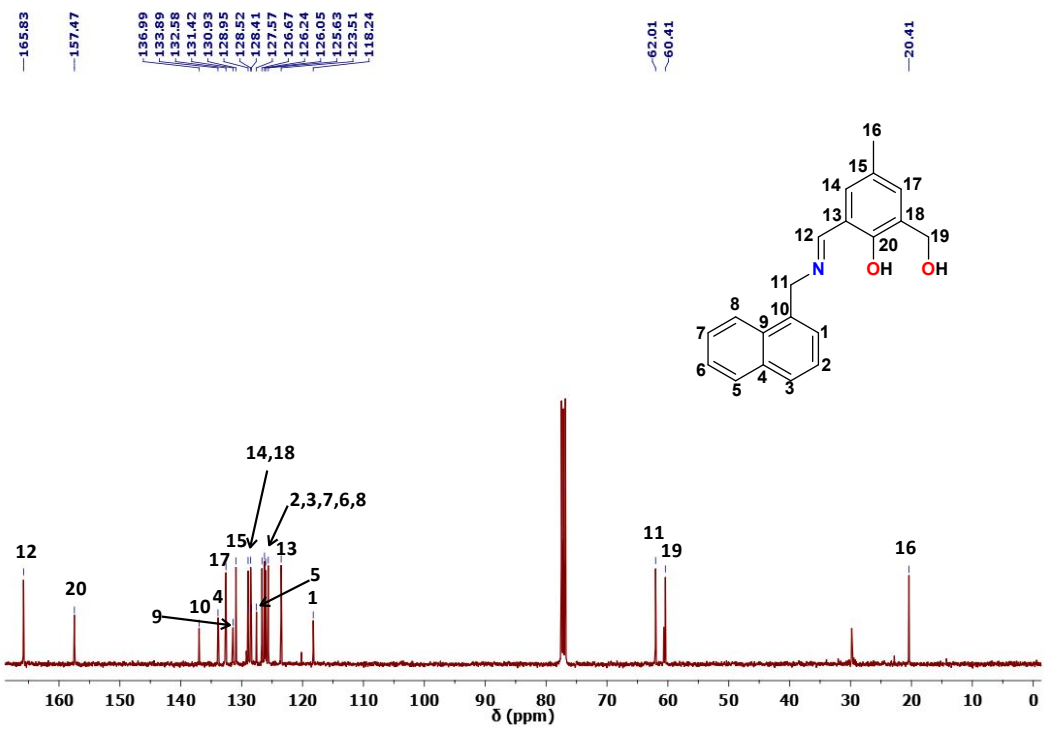

Figure S10. ^{13}C NMR spectrum of chemosensor **L2** in $CDCl_3$.

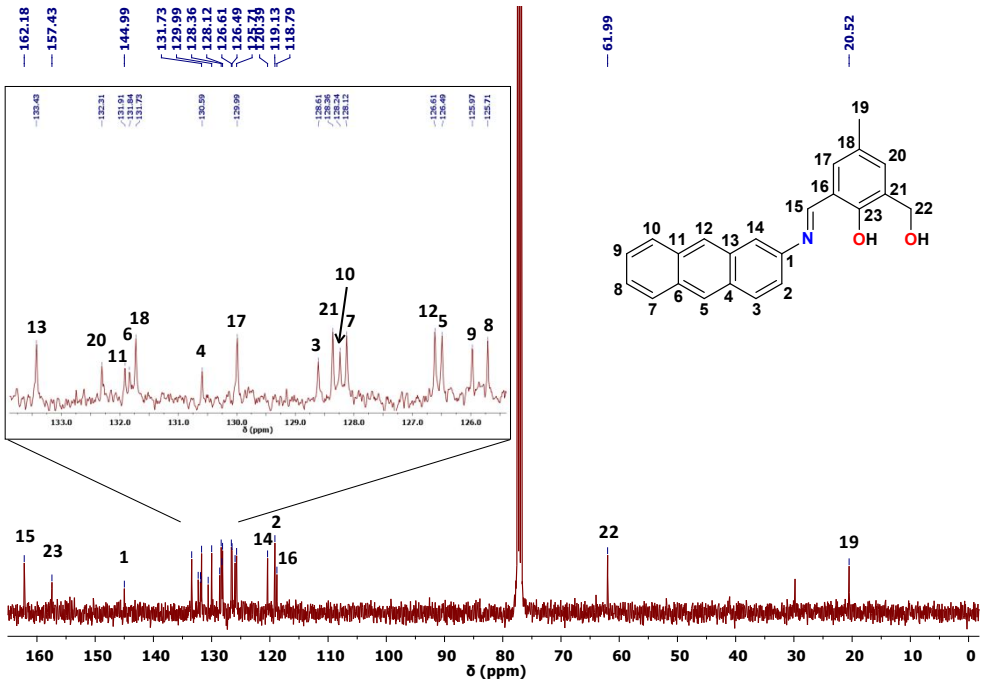

Figure S11. ^{13}C NMR spectrum of chemosensor **L3** in $CDCl_3$.

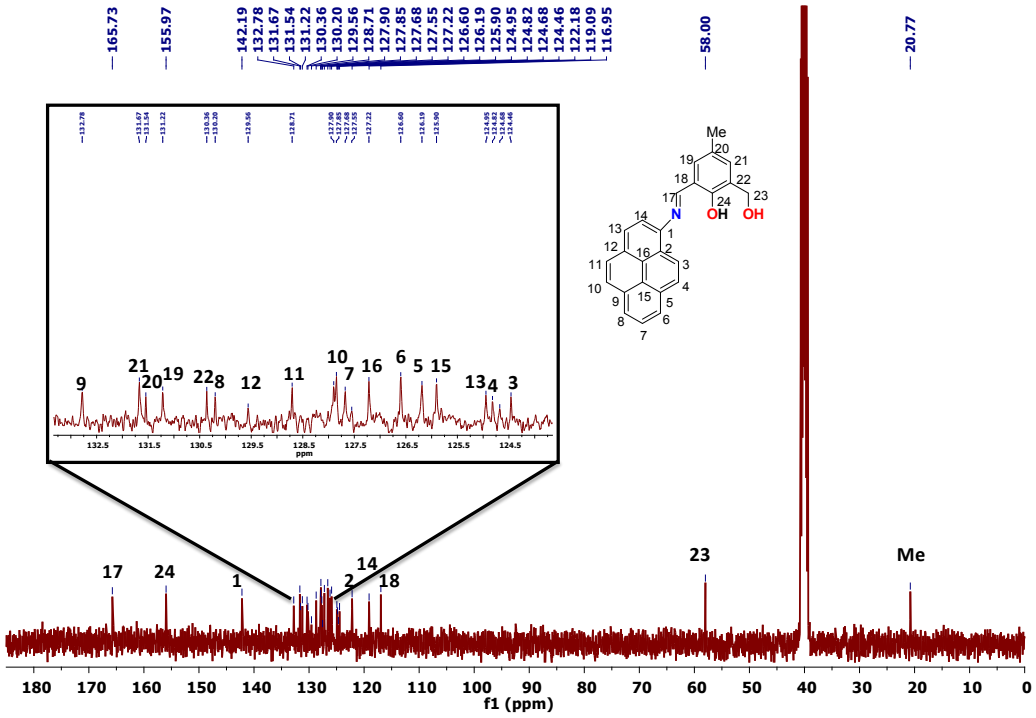

Figure S12. ^{13}C NMR spectrum of chemosensor **L4** in DMSO-d6.

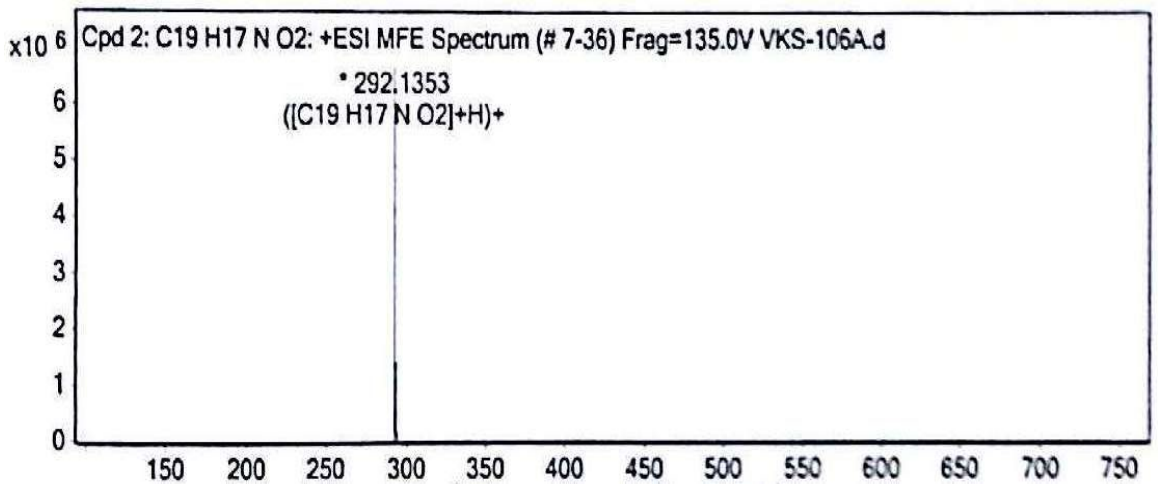

Figure S13. ESI$^+$ HR mass spectrum of chemosensor **L1** recorded in CH_3OH.

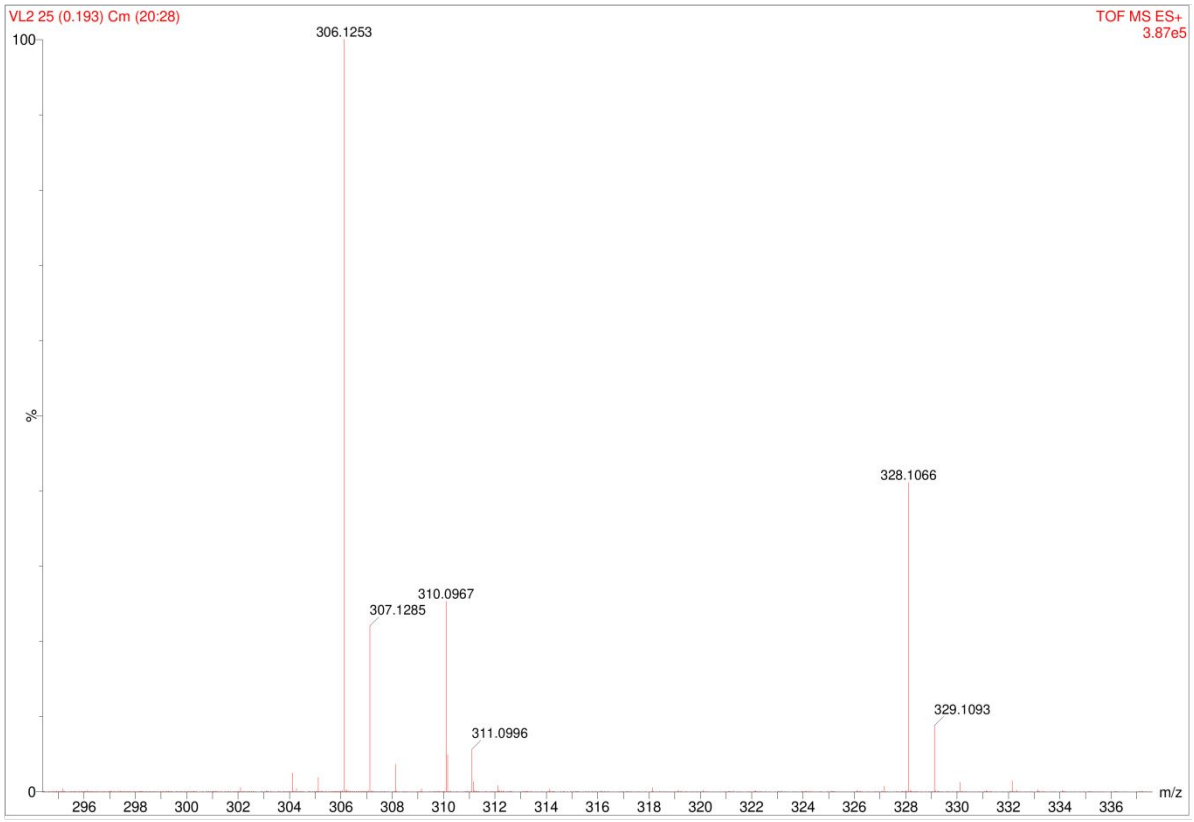

Figure S14. ESI$^+$ HR mass spectrum of chemosensor **L2** recorded in CH_3OH.

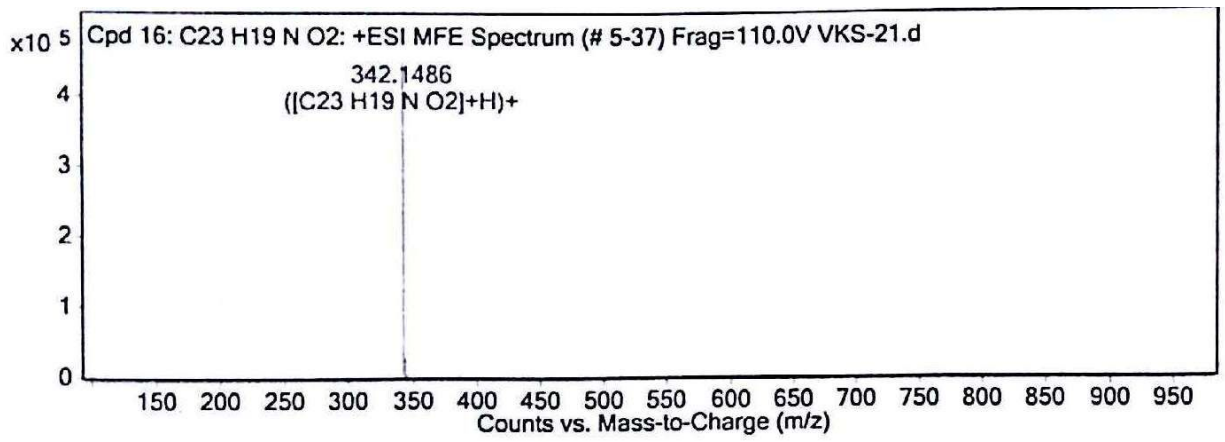

Figure S15. ESI^+ HR mass spectrum of chemosensor **L3** recorded in CH_3OH.

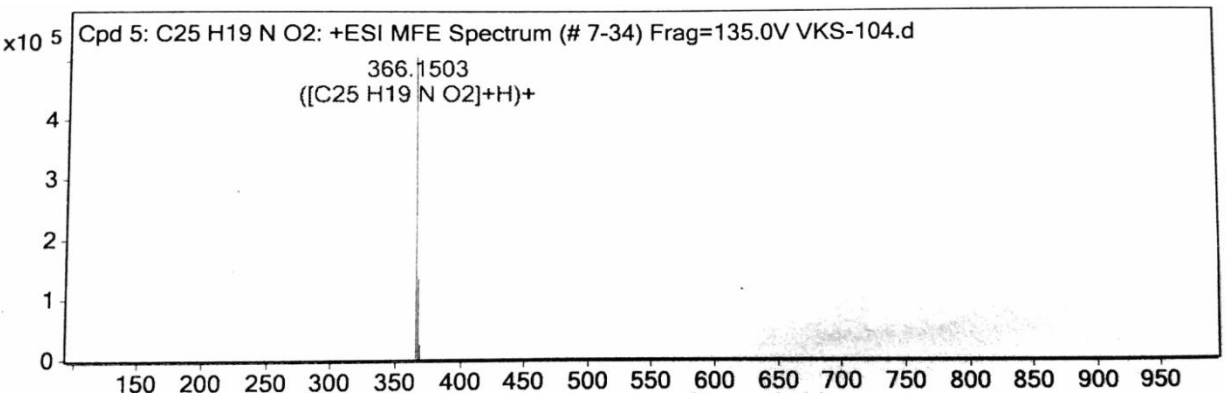

Figure S16. ESI^+ mass spectrum of chemosensor **L4** recorded in CH_3OH.

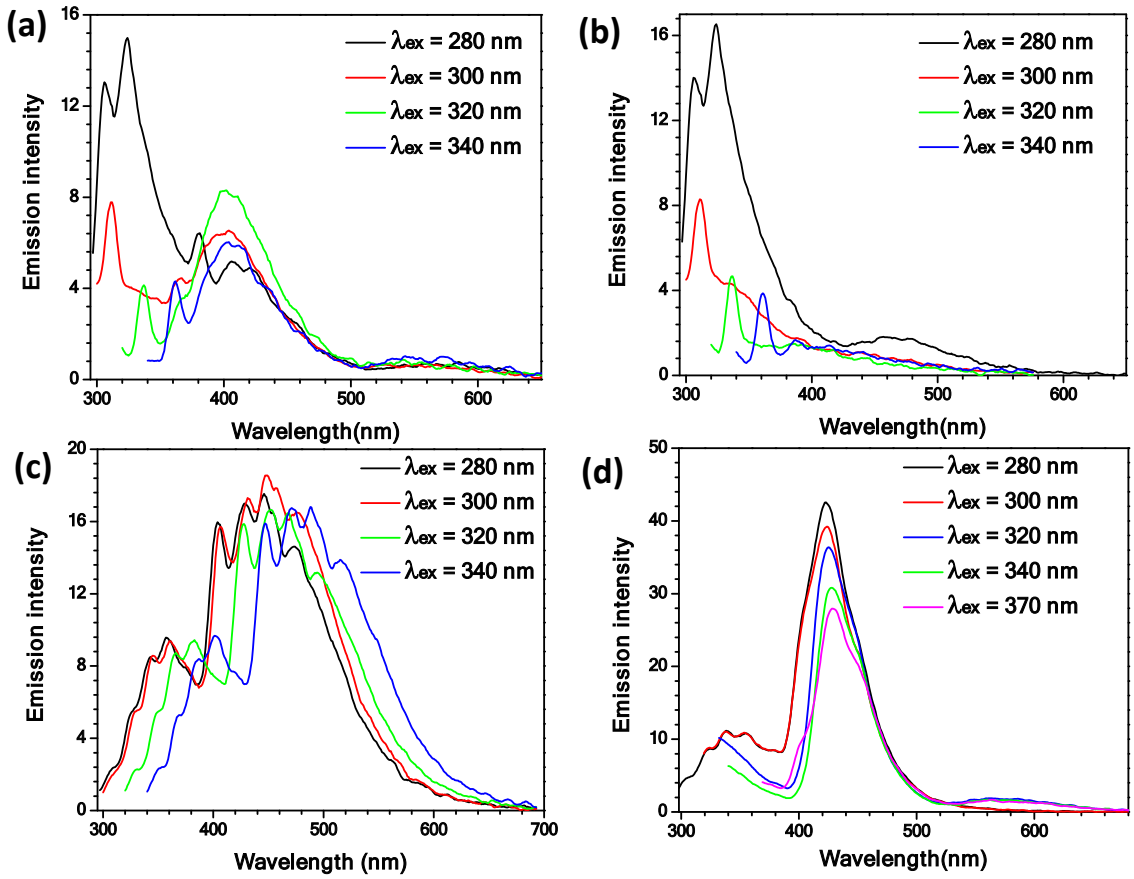

Figure S17. Emission spectra of chemosensors **L1–L4** (5 μM) recorded in EtOH (containing 0.5% THF) after exciting at different wavelengths.

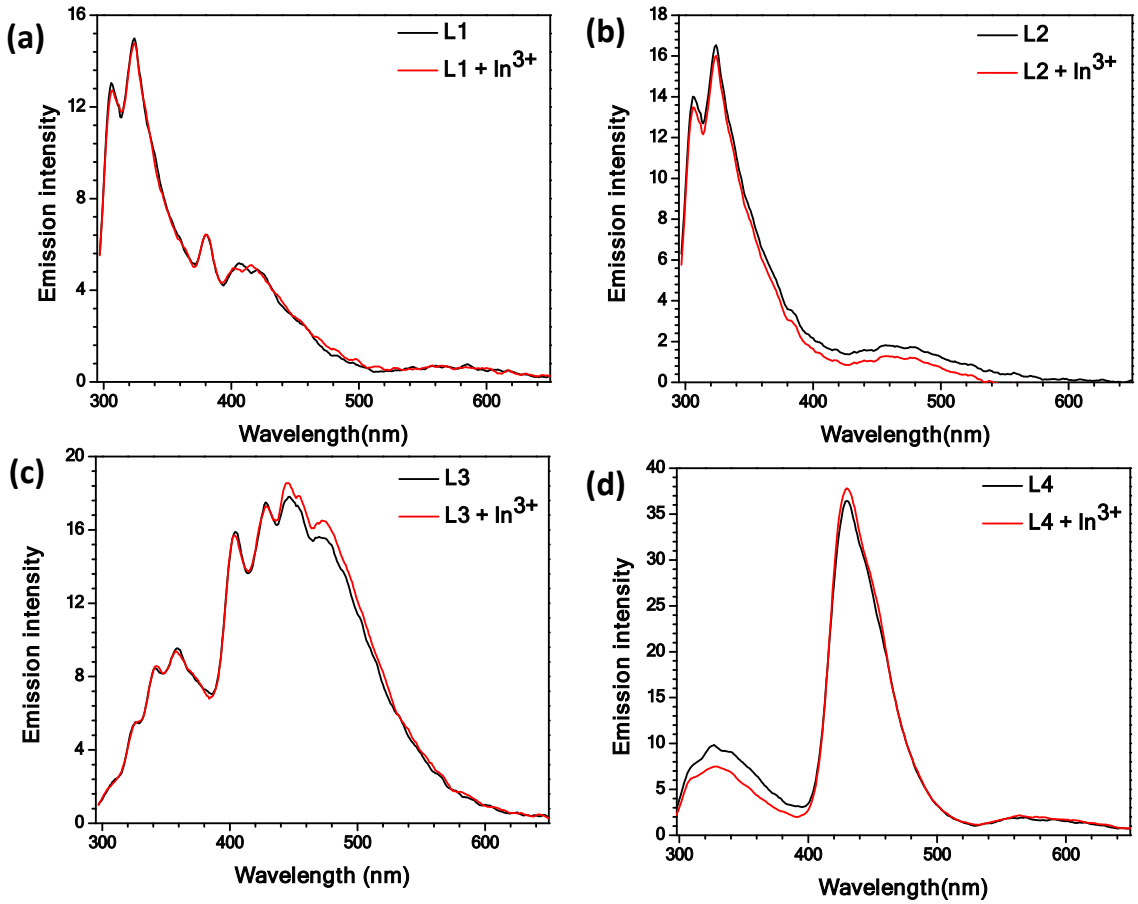

Figure S18. Change in emission spectra of chemosensors **L1–L4** (5 μM) in presence of 10 equivalents of In^{3+} ion in EtOH (containing 0.5% THF); (a) **L1**, (b) **L2**, (c) **L3** and (d) **L4.**

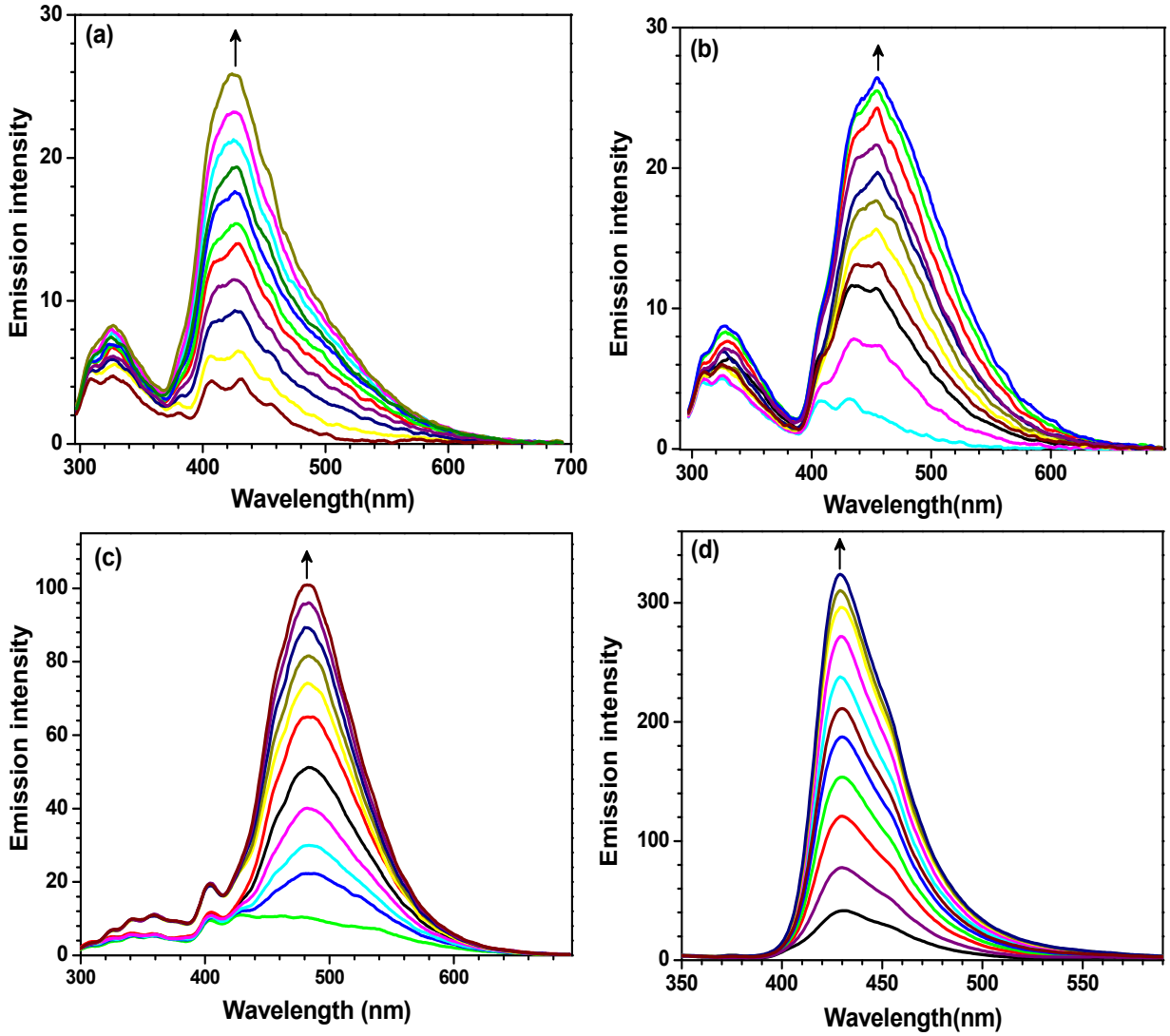

Figure S19. Change in emission spectra of chemosensors **L1-L4** (5 μM) in presence of 10 equivalents of Al^{3+} ion in EtOH (containing 0.5% THF); (a) **L1** (b) **L2** (c) **L3** and (d) **L4**.

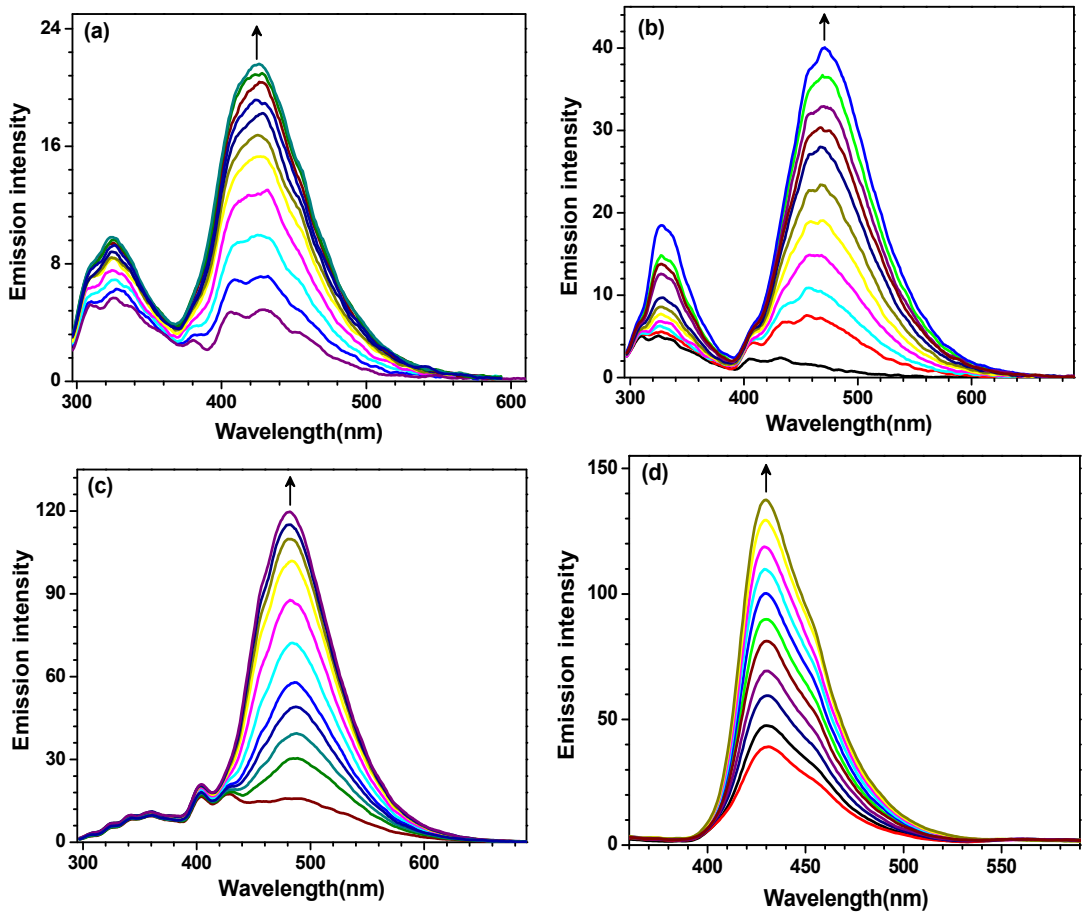

Figure S20. Change in emission spectra of chemosensors **L1-L4** (5 μM) in presence of 10 equivalents of Ga^{3+} ion in EtOH (containing 0.5% THF); (a) **L1** (b) **L2** (c) **L3** and (d) **L4**.

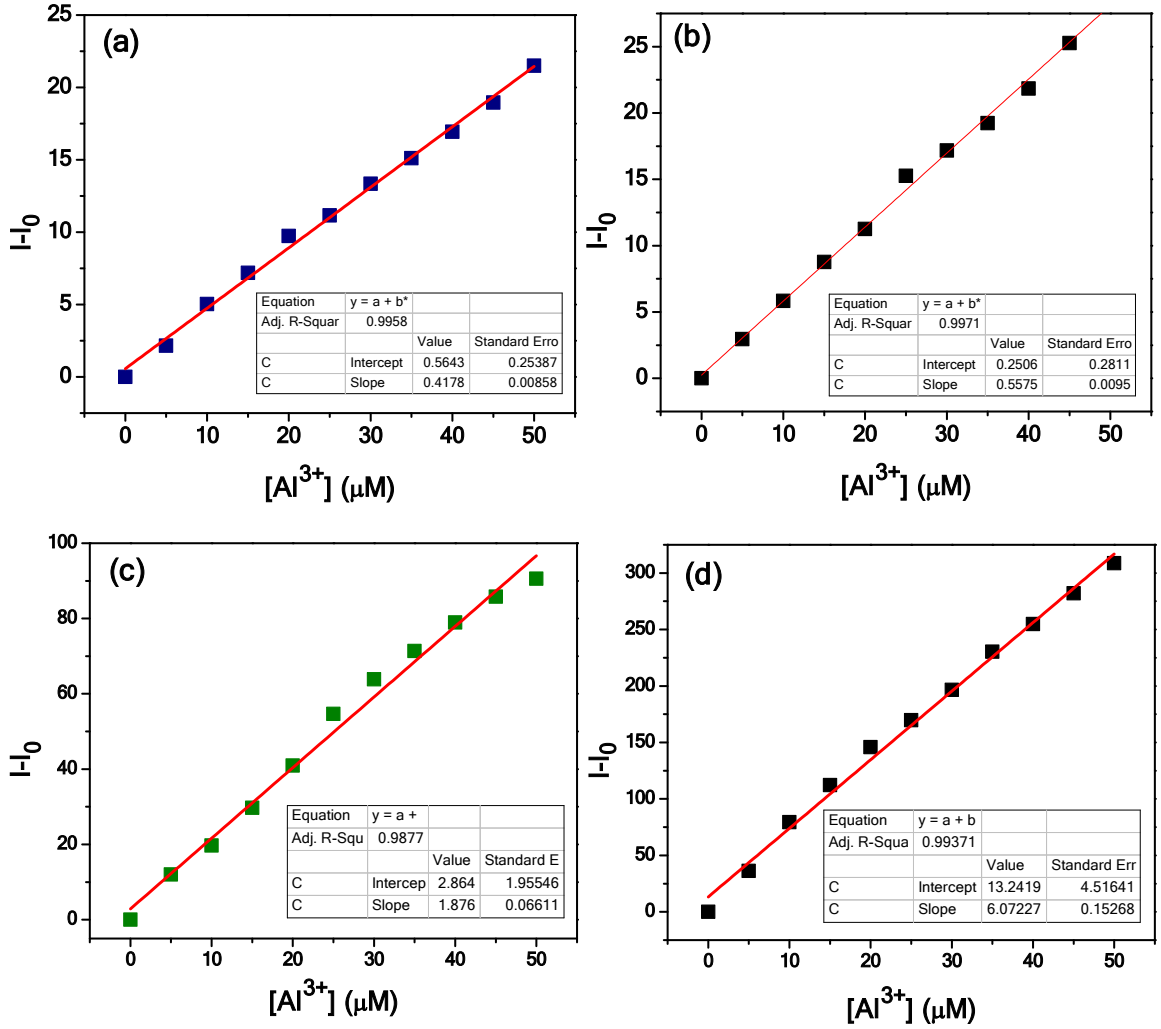

Figure S21. Determination of detection limits for the detection of Al^{3+} ion by chemosensors (a) **L1**; (b) **L2**; (c) **L3** and (d) **L4** from emission spectral changes recorded in EtOH (containing 0.5% THF).

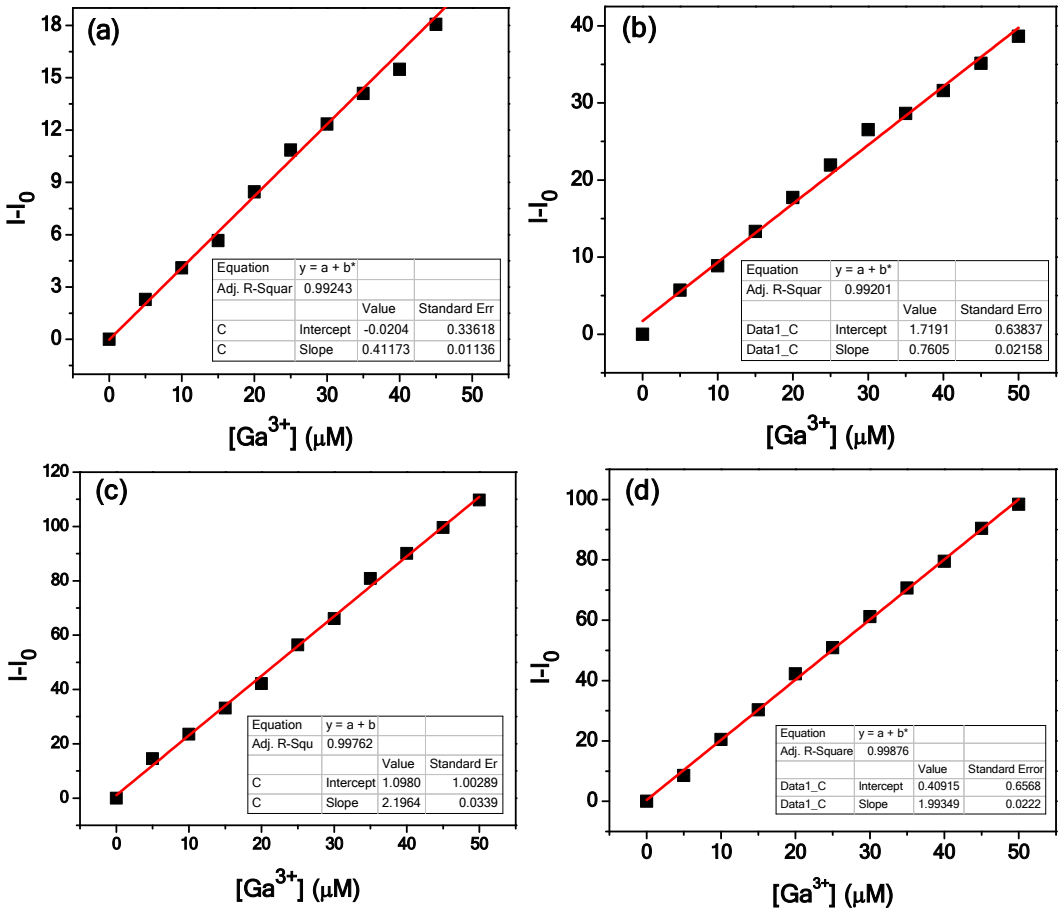

Figure S22. Determination of detection limits for the detection of Ga^{3+} ion by chemosensors (a) **L1**; (b) **L2**; (c) **L3** and (d) **L4** from emission spectral changes recorded in EtOH (containing 0.5% THF).

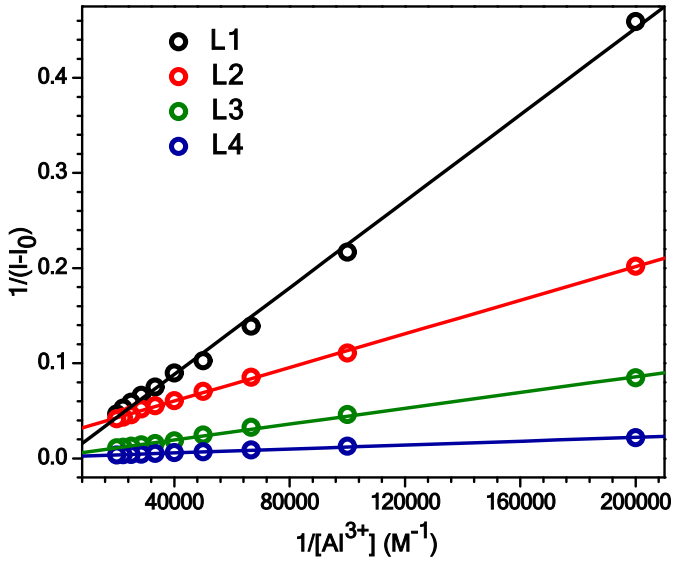

Figure S23. Benesi-Hildebrand plots for the detection of Al^{3+} ion by chemosensors **L1-L4** (5 μM).

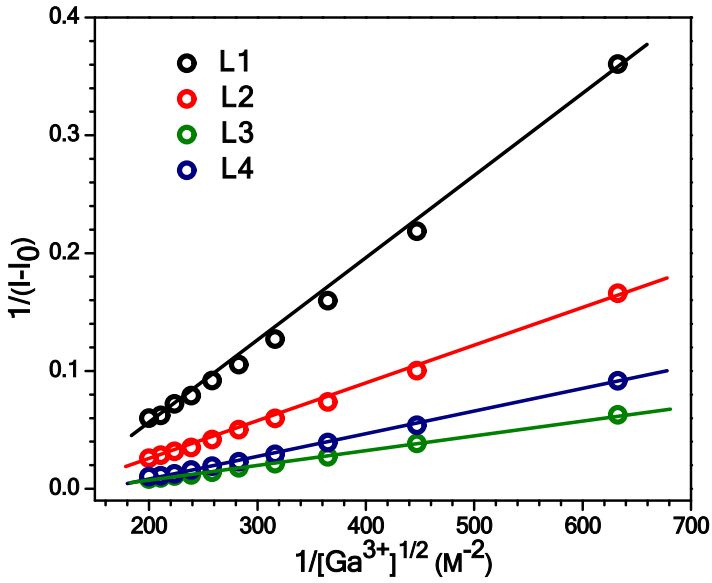

Figure S24. Benesi-Hildebrand plots for the detection of Ga^{3+} ion by chemosensors **L1-L4** (5 μM).

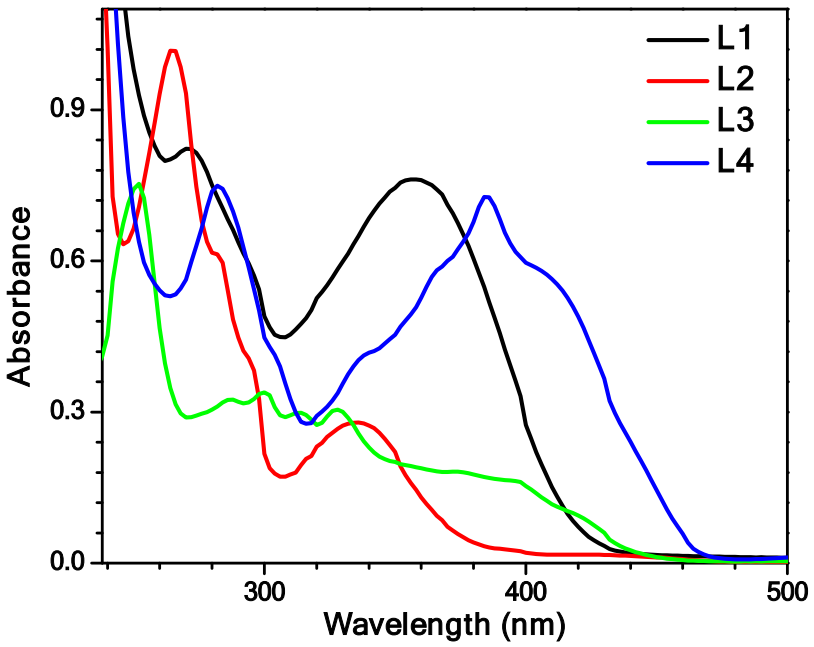

Figure S25. UV-Vis spectra of chemosensors **L1-L4** (5 μM) in EtOH (containing 0.5% THF).

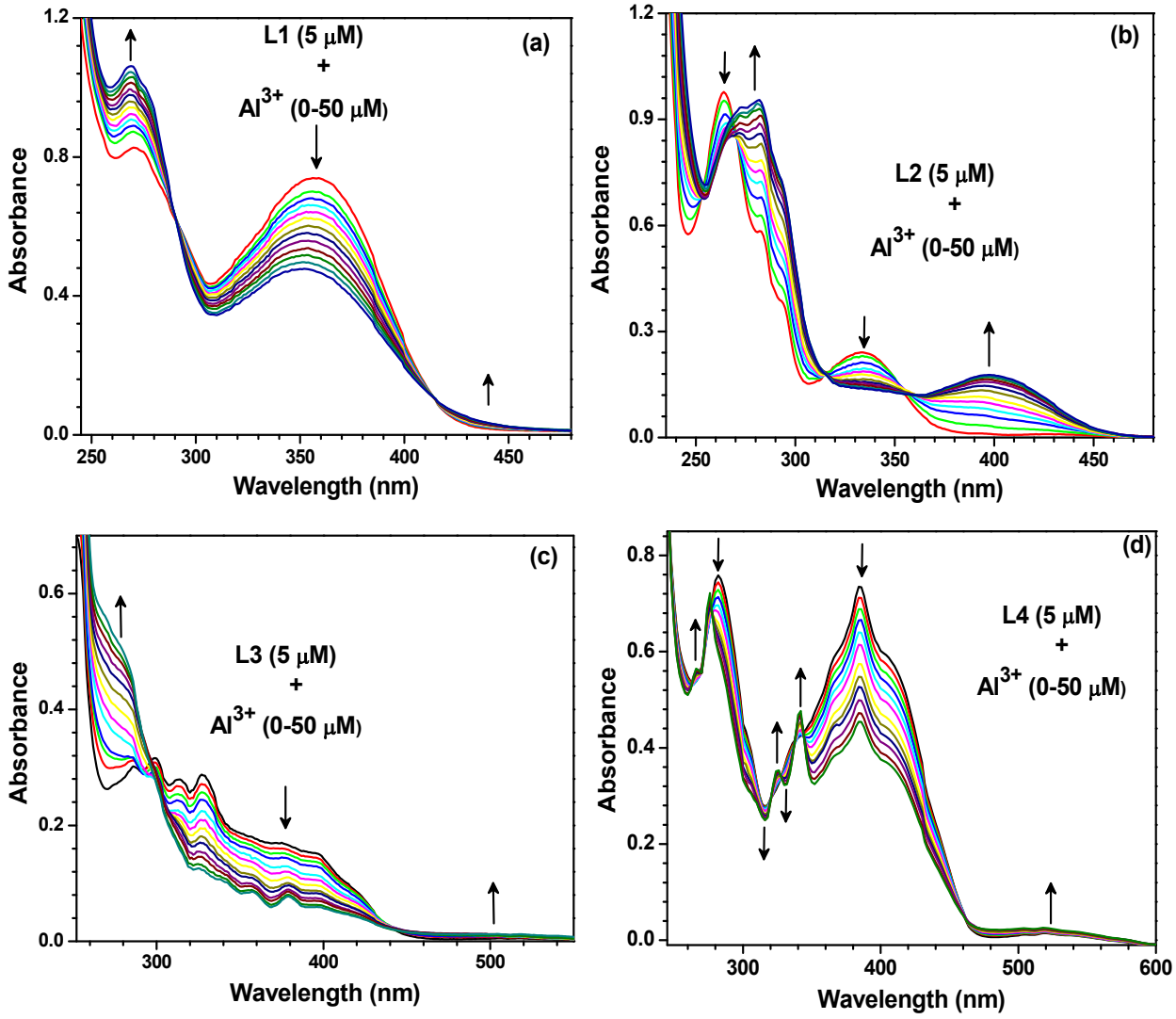

Figure S26. Change in absorption spectra of chemosensors **L1-L4** (5 μM) in presence of 10 equivalents of Al^{3+} ion in EtOH (containing 0.5% THF); (a) **L1** (b) **L2** (c) **L3** and (d) **L4**.

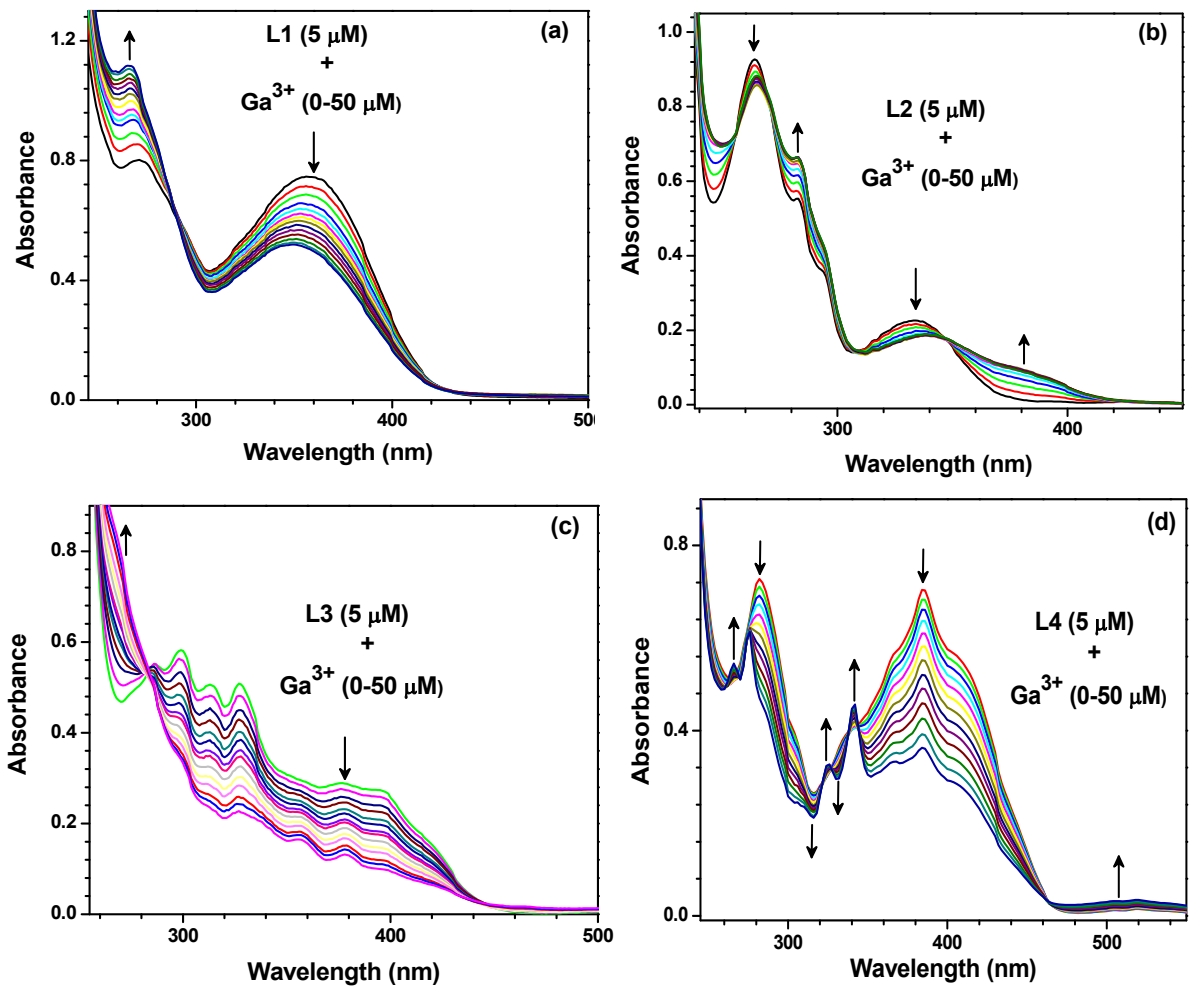

Figure S27. Change in absorption spectra of chemosensors **L1-L4** (5 μM) in presence of 10 equivalents of Ga^{3+} ion in EtOH (containing 0.5% THF); (a) **L1** (b) **L2** (c) **L3** and (d) **L4**.

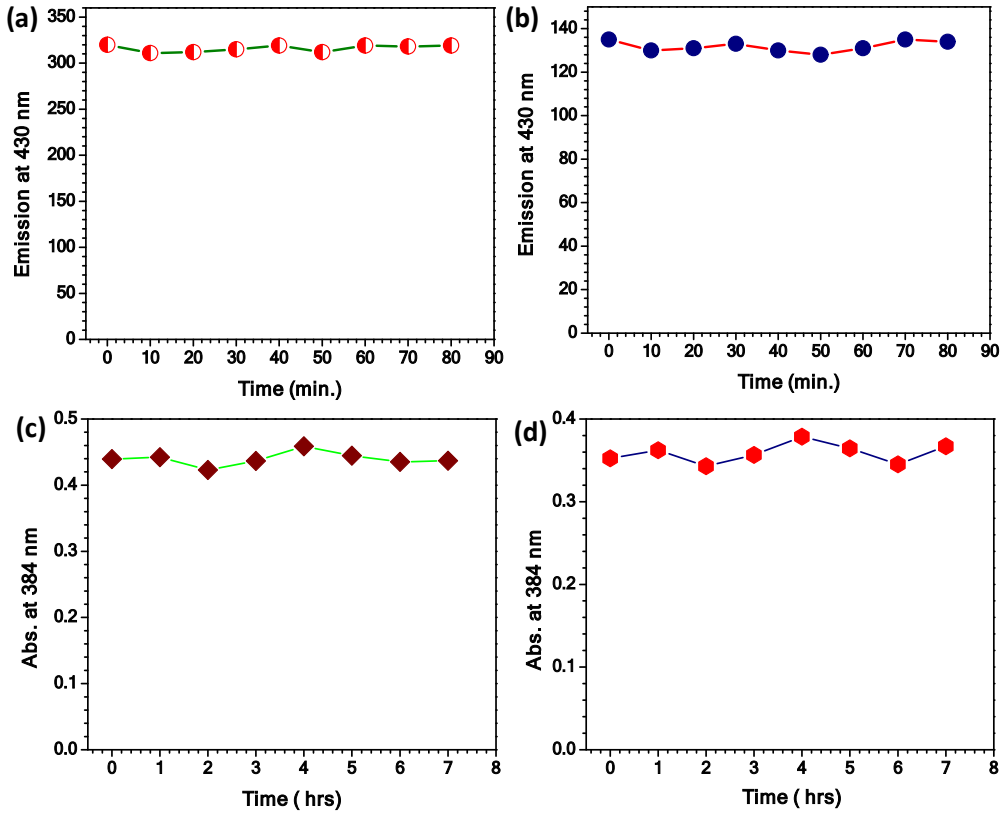

Figure S28. Evaluation of stability of **L4**–Al^{3+} species by (a) fluorescence and (b) absorption spectral studies. Evaluation of stability of **L4**–Ga^{3+} species by (c) fluorescence and (d) absorption spectral studies. Studies have been done in EtOH-H_2O (1:1 v/v).

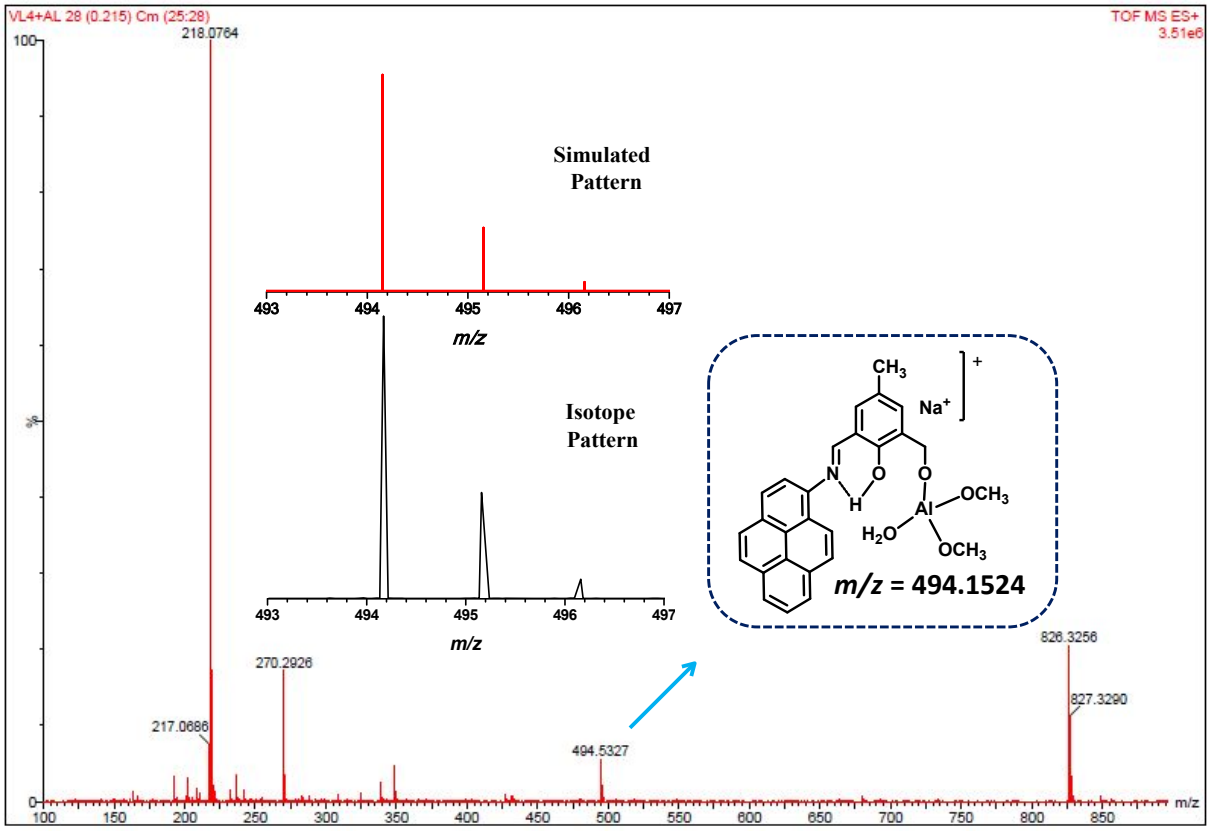

Figure S29. ESI$^+$ HR mass spectrum of **L4**-Al^{3+} in CH_3OH along with the simulated pattern.

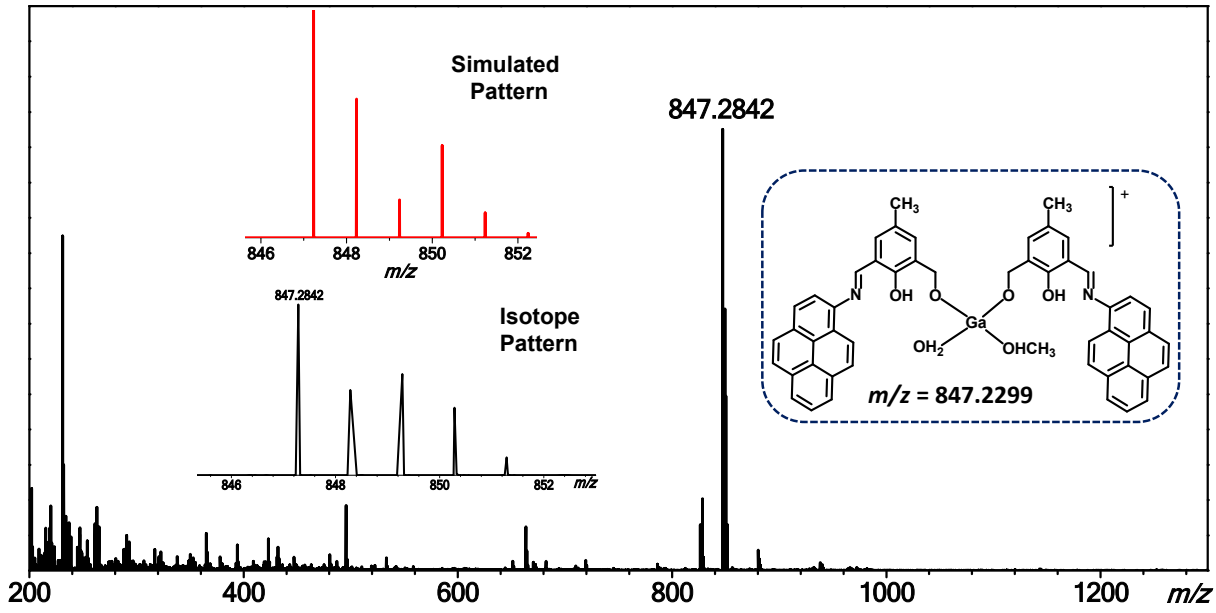

Figure S30. ESI$^+$ HR mass spectrum of **L4**-Ga^{3+} in CH_3OH along with the simulated pattern.

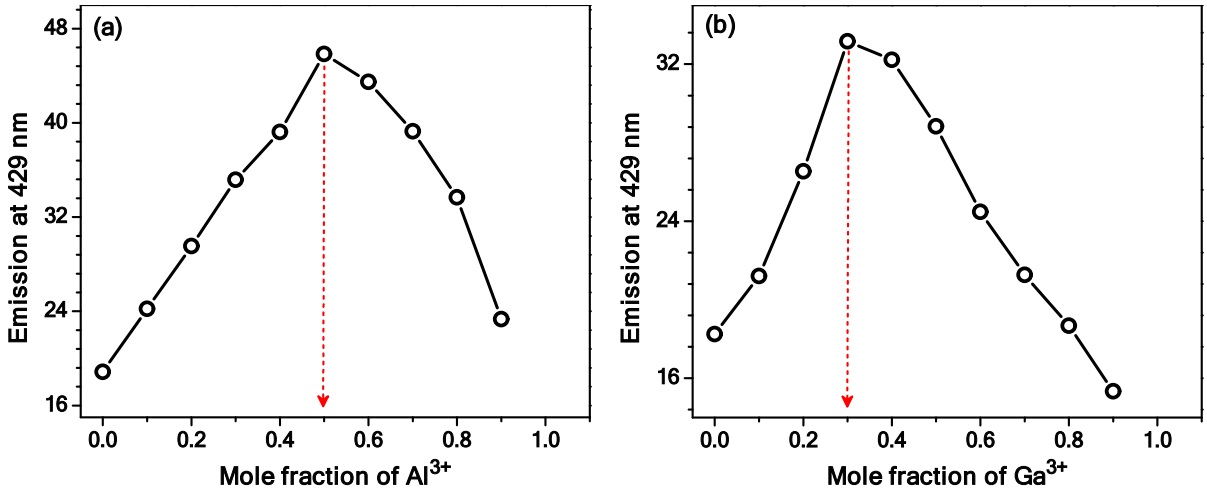

Figure S31. Job's plot for the detection of (a) Al^{3+} and (b) Ga^{3+} ions by chemosensor **L4** in EtOH (containing 0.5% THF).

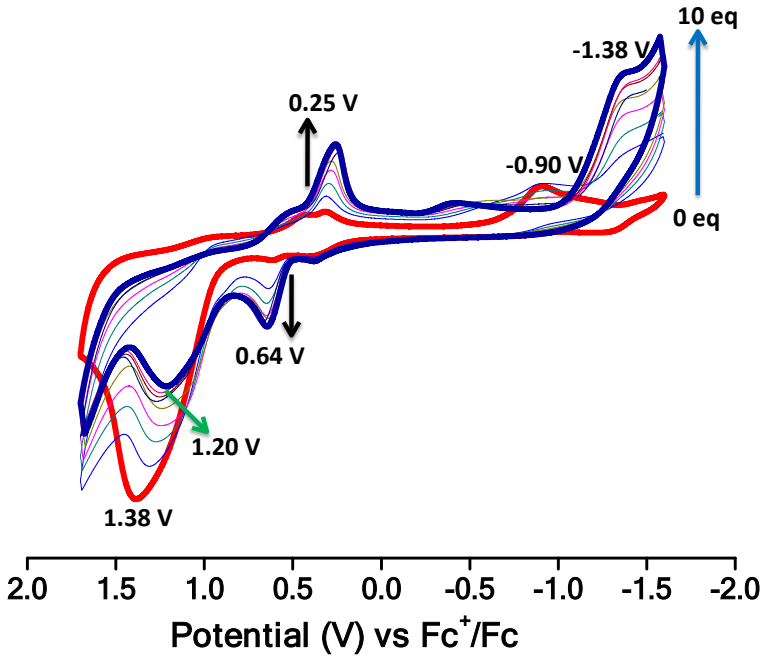

Figure S32. Cyclic voltammetric titrations of chemosensor **L4** (EtOH, 2.5 mM) after the incremental addition (1 – 10 equivalents) of $Al(NO_3)_3$ (0 – 25 mM). Conditions: solvent, EtOH; supporting electrolyte, tetrabutyl ammonium perchlorate (TBAP); working electrode, glassy carbon; reference electrode, Ag/Ag^+; scan rate, 100 mV/s.

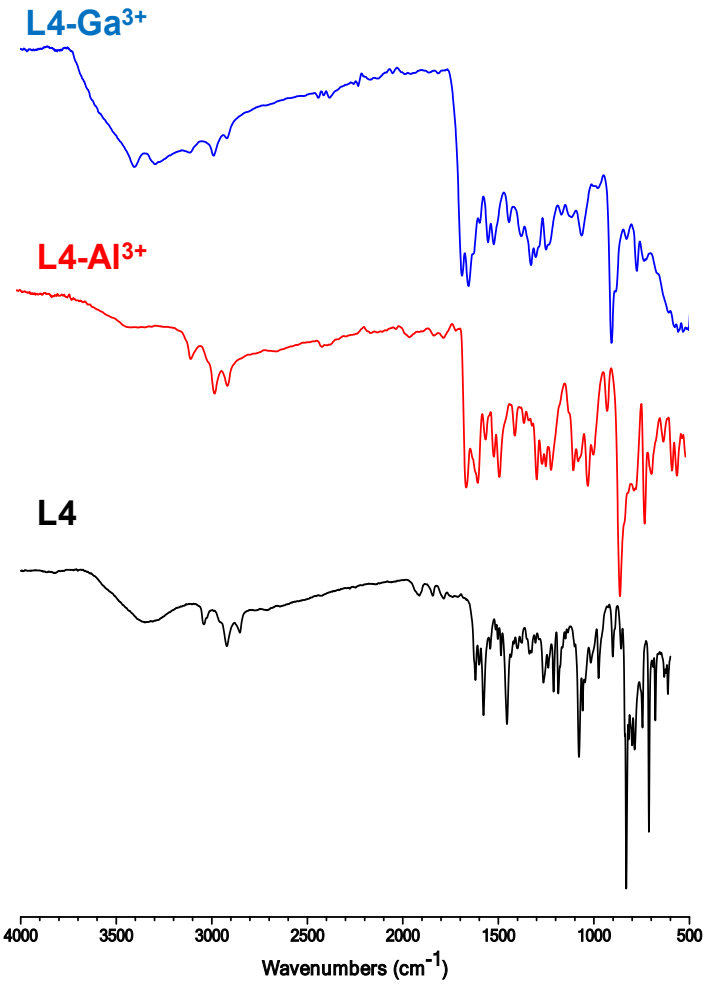

Figure S33. FTIR spectra of **L4**, **L4**-Al^{3+} and **L4**-Ga^{3+}.

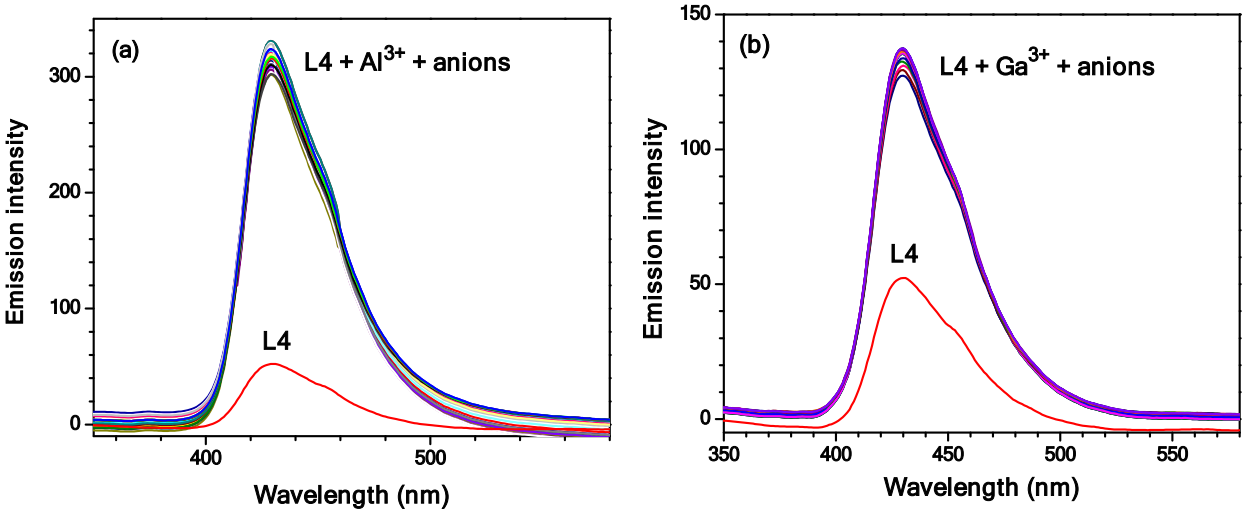

Figure S34. Effect of different anions on the emission of (a) **L4**-Al^{3+} and (b) **L4**-Ga^{3+} in EtOH (containing 0.5% THF) and their comparison with chemosensor **L4**.

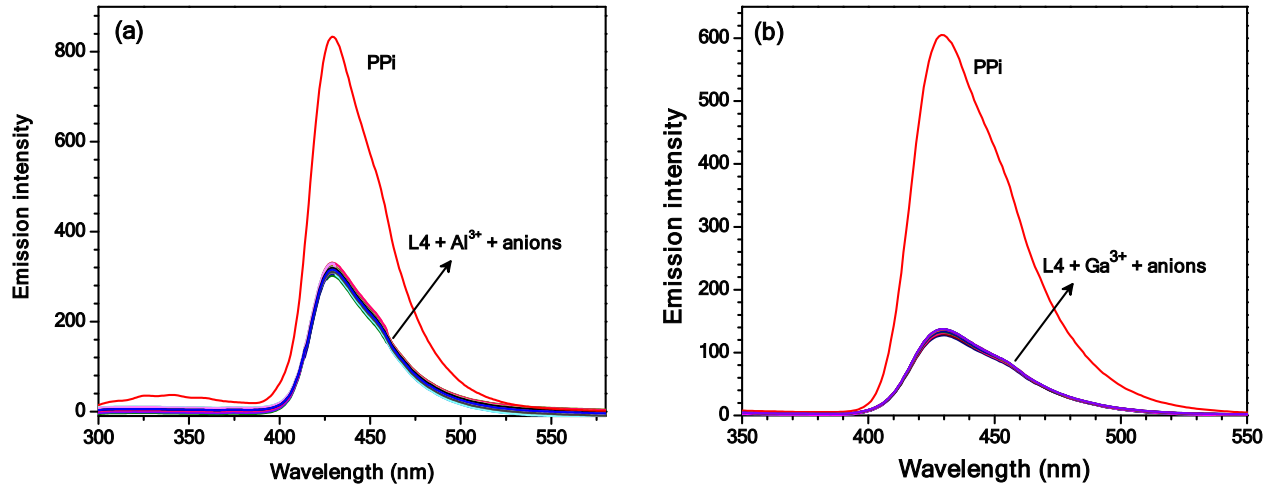

Figure S35. Effect of different anions including PPi on the emission of (a) **L4**-Al^{3+} and (b) **L4**-Ga^{3+} species in EtOH (containing 0.5% THF).

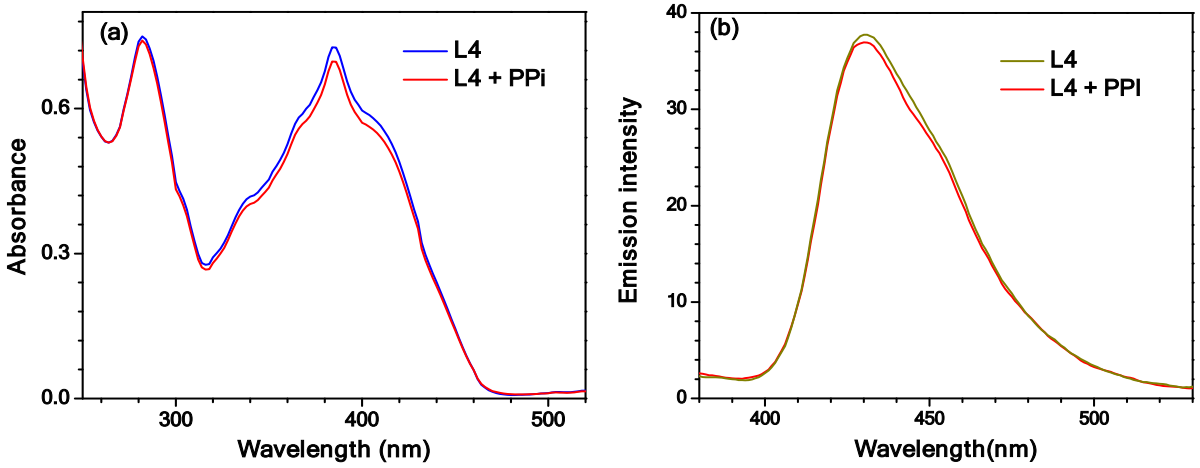

Figure S36. (a) UV-Vis spectrum of chemosensor **L4** (5 μM) in presence of PPi (10 equivalents) in EtOH (containing 0.5% THF). (b) Emission spectrum of chemosensor **L4** (5 μM) in presence of PPi (10 equivalents) in EtOH (containing 0.5% THF).

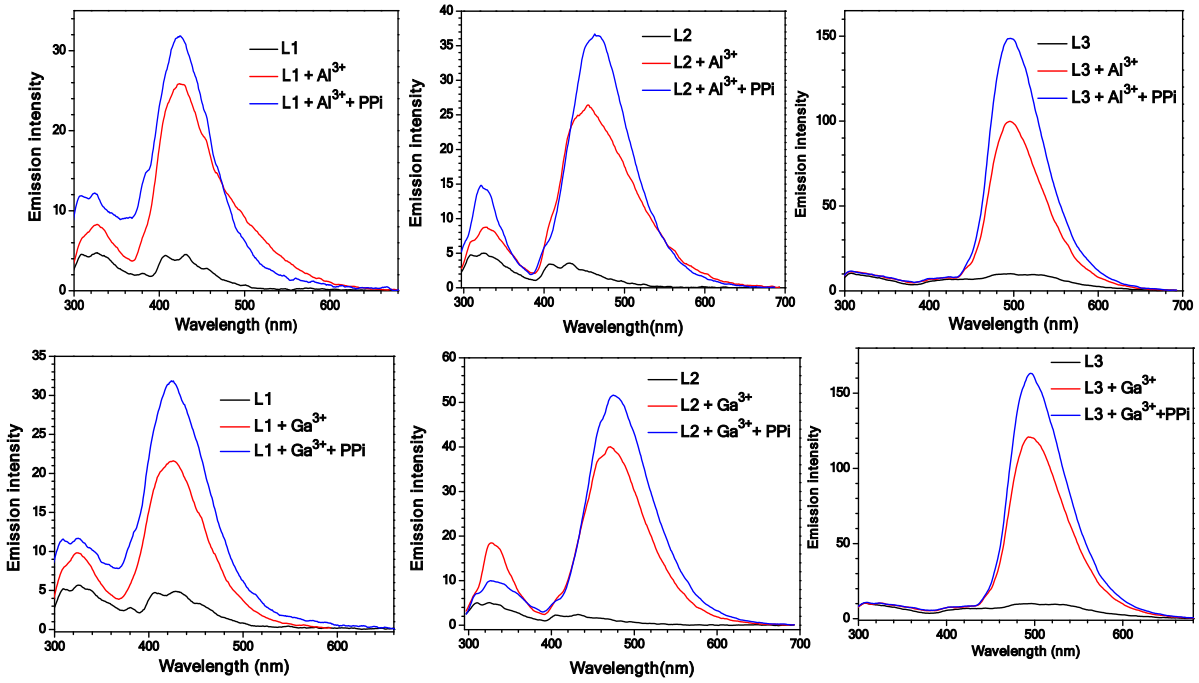

Figure S37. Effect of PPi (10 equivalents) in presence of Al^{3+}/Ga^{3+} ions (10 equivalents) on the emission spectra of chemosensors **L1-L3** (5 μM) in EtOH (containing 0.5% THF).

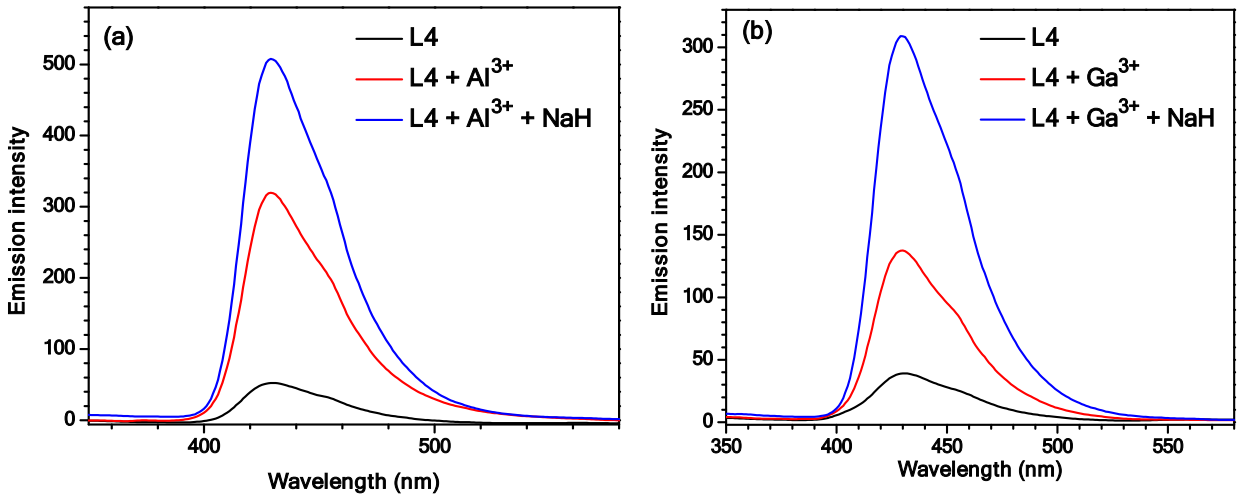

Figure S38. Effect of Al^{3+}/Ga^{3+} ions (10 equivalents) and NaH (10 equivalents) on the emission spectra of chemosensor **L4** (5 μM) in EtOH (containing 0.5% THF).

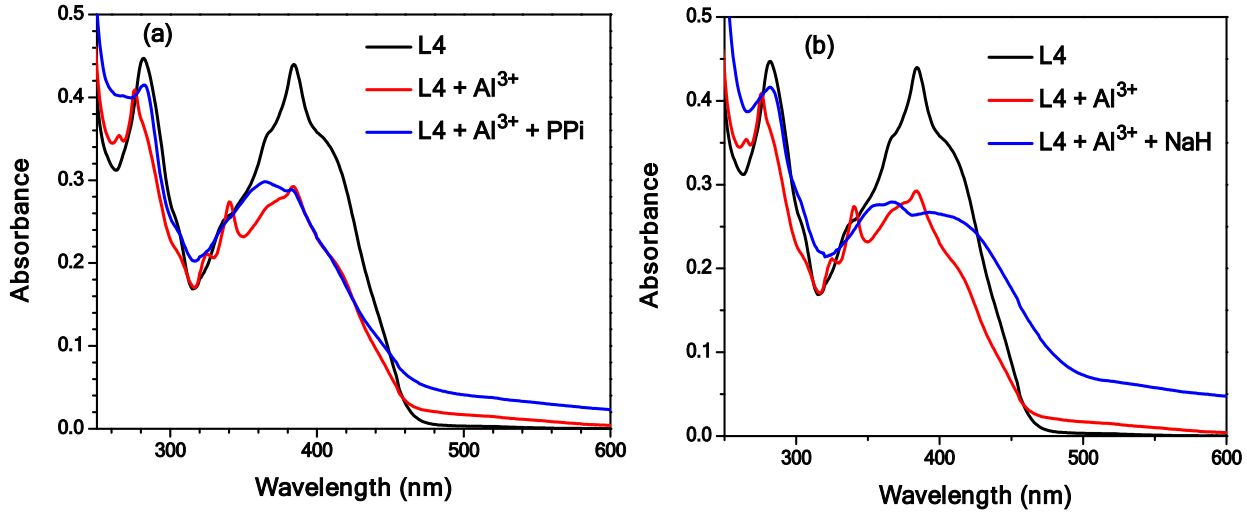

Figure S39. UV-Vis spectra of (a) **L4**, **L4** + Al^{3+} (10 equivalents) and **L4** + Al^{3+} (10 equivalents) + PPi (10 equivalents) (b) **L4**, **L4** + Al^{3+} (10 equivalents) and **L4** + Al^{3+} (10 equivalents) + NaH (10 equivalents) in EtOH (containing 0.5% THF).

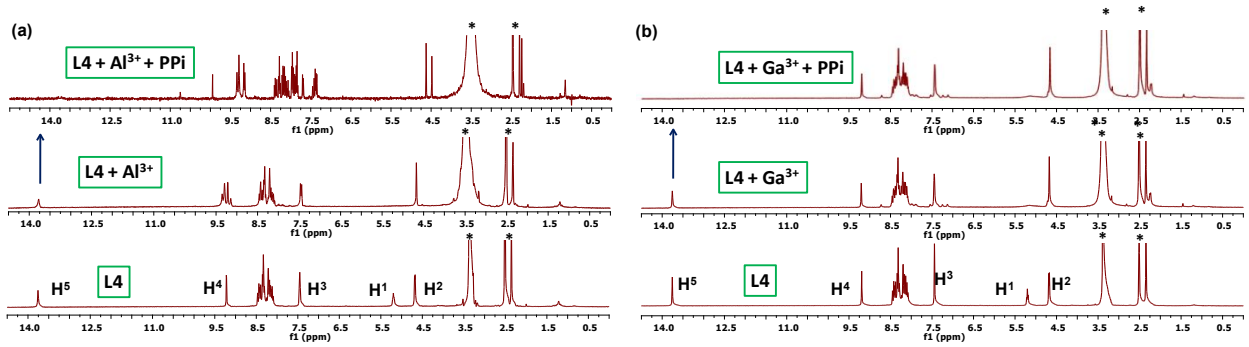

Figure S40.[1]H NMR spectra of chemosensor **L4** (2.0 mM, DMSO-d[6]) in the absence and presence of (a) Al^{3+} ion (10 equivalents) and PPi (10 equivalents); (b) Ga^{3+} ion (10 equivalents) and PPi (10 equivalents); * represents the residual solvent and/or adventitious water peaks.

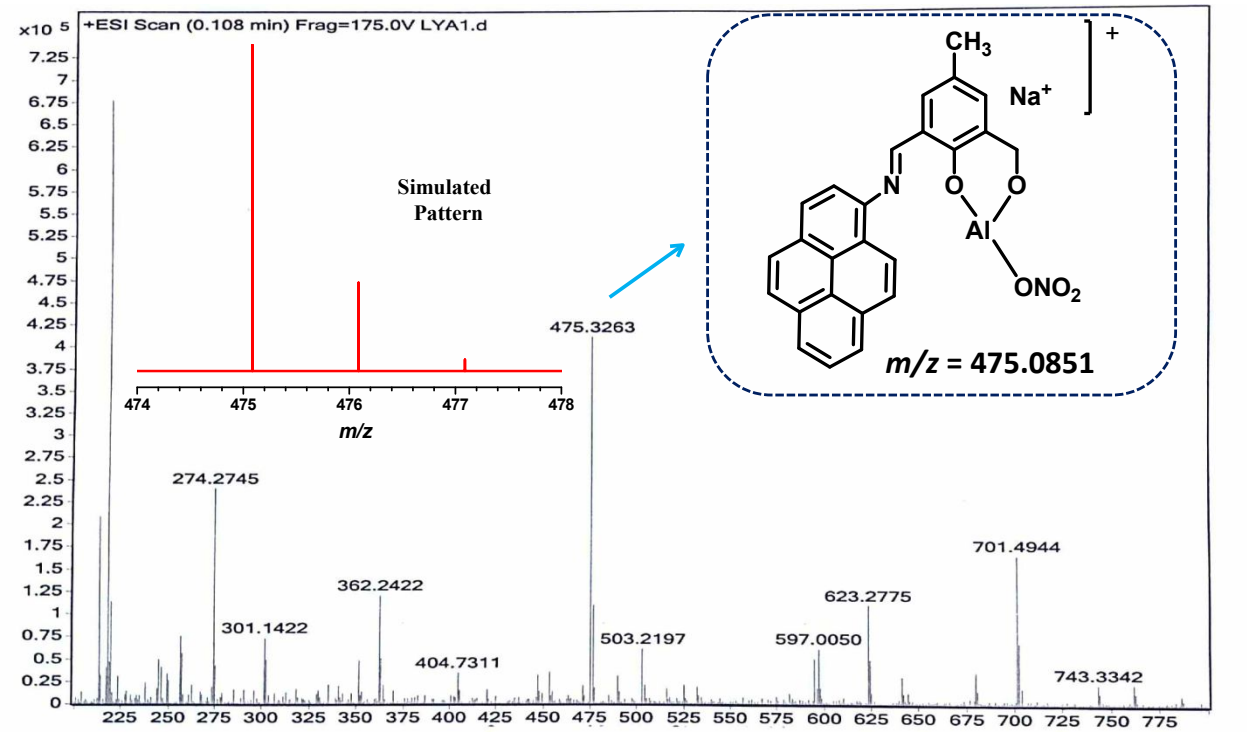

Figure S41. ESI^+ HR mass spectrum of **L4-Al^{3+}** in presence of PPi in CH_3OH and its simulation pattern.

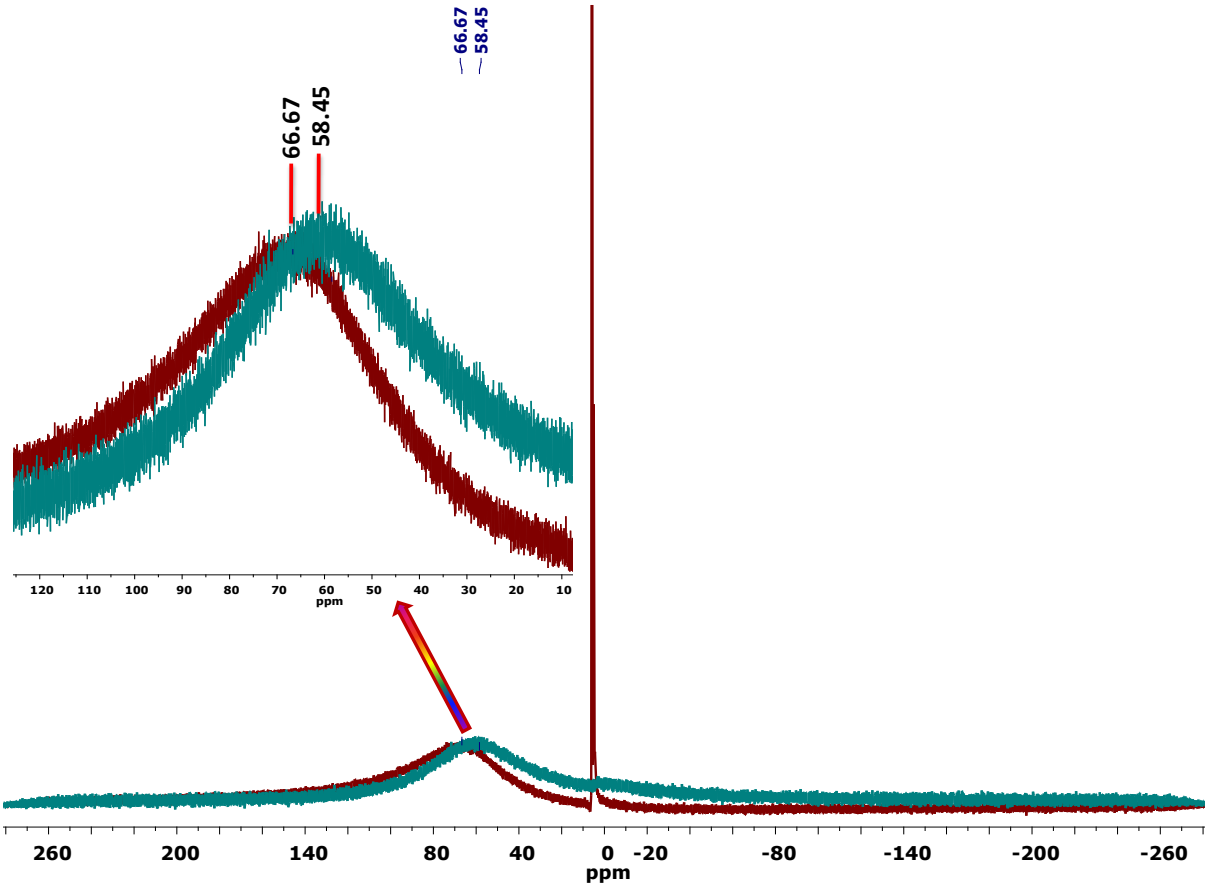

Figure S42. ^{27}Al-NMR spectrum for the solution generated [**L4**+Al^{3+}] species (brown trace) after the addition of 10 equivalents of $Al(NO_3)_3$ to chemosensor **L4** and after the subsequent addition of 10 equivalents of PPi (teal trace). All studies have been done in DMSO-d_6.

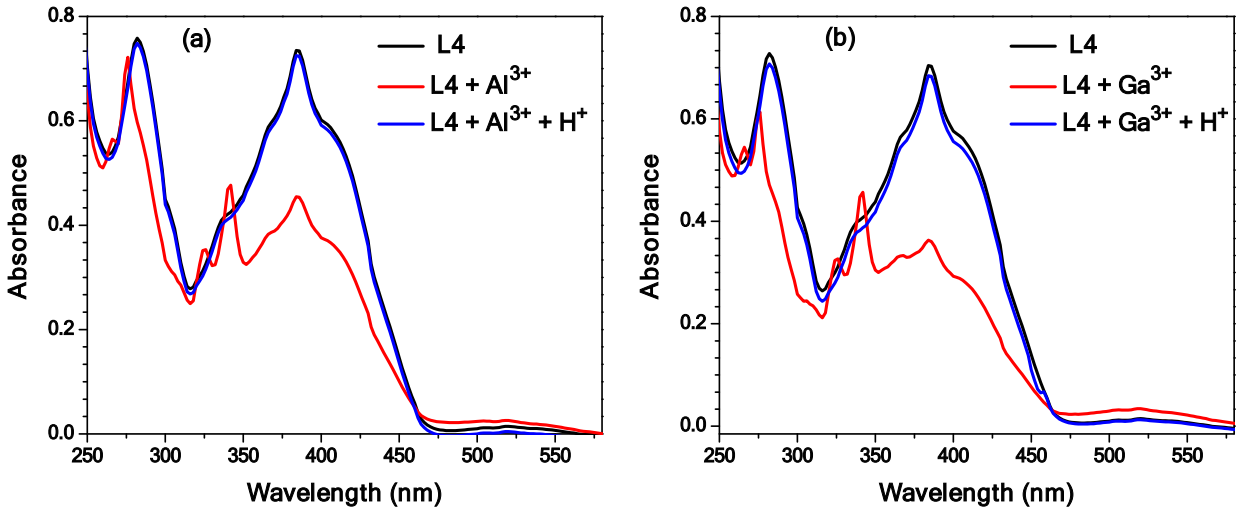

Figure S43. UV-vis spectra of (a) **L4**, **L4** + Al^{3+} (10 equivalents) and **L4** + Al^{3+} (10 equivalents) + H^{+} (10 equivalents) (b) **L4**, **L4** + Ga^{3+} (10 equivalents) and **L4** + Ga^{3+} (10 equivalents) + H^{+} (10 equivalents) in EtOH (containing 0.5% THF).

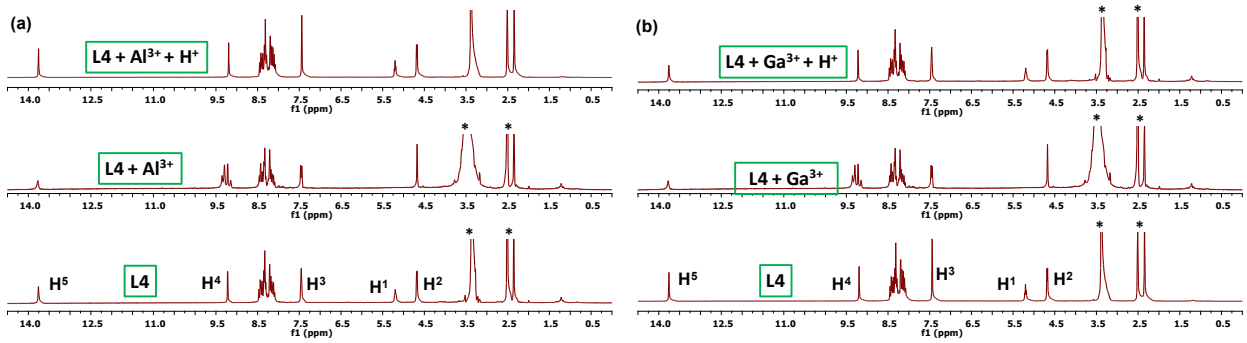

Figure S44. ^{1}H NMR spectra of chemosensor **L4**: (a) **L4**, L4 + Al^{3+} (10 equivalents) and L4 + Al^{3+} (10 equivalents) + H^{+} (10 equivalents) (b) **L4**, L4 + Ga^{3+} (10 equivalents) and L4 + Ga^{3+} (10 equivalents) + H^{+} (10 equivalents) in DMSO-d_6.

Table S1. Crystallographic data collection and structure solution parameters for chemosensor **L1**.

Empirical formula	$C_{19}H_{17}NO_2$
Formula weight	291.33
Temperature/K	293(2)
Crystal system	monoclinic
Space group	I_2/a
a/Å	16.2485(12)
b/Å	3.9567(3)
c/Å	47.433(4)
α/°	90
β/°	98.011(8)
γ/°	90
Volume/Å^3	3019.7(4)
Z	8
ρ_{calc}mg/mm^3	1.282
m/mm^{-1}	0.083
F(000)	1232
Crystal size/mm^3	0.26 × 0.22 × 0.1
Theta range for data collection	6.526 to 49.996°
Index ranges	$-19 \leq h \leq 19$, $-4 \leq k \leq 4$, $-56 \leq l \leq 56$
Reflections collected	16492
Independent reflections	2656 [R(int) = 0.0642]
Data/restraints/parameters	2656/1/219
Goodness-of-fit on F^2	0.993
Final R indexes [I>2σ (I)]	R_1 = 0.0613, wR_2 = 0.1414
Final R indexes [all data]	R_1 = 0.1132, wR_2 = 0.1685
Largest diff. peak/hole / e Å^{-3}	0.214/-0.157
CCDC No.	1895256

Table S2. A comparison of the sensing performance of selected chemosensors for the detection of Al^{3+} ion.

S. No.	Chemosensor	Solvent(s)/Buffer	Detection limit for Al^{3+} ion	Reference
1	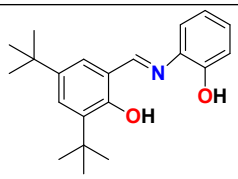	HEPES buffer (20 mM, 1% EtOH, pH = 7.04)	0.0294 μM	Liang, C.; Bu, W.; Li, C.; Men, G.; Deng, M.; Jiangyao, Y.; Sunb, H.; Jiang, S. *Dalton Trans.*, **2015**, *44*, 11352.
2	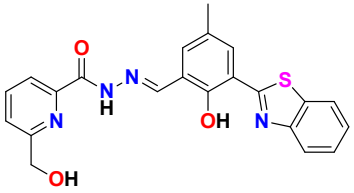	CH_3OH/H_2O	0.0672 μM	Das, S.; Goswami, S.; Aich, K.; Ghoshal, K.; Quah, C. K.; Bhattacharya, M.; Funcd, H. *New J. Chem.*, **2015**, ***39***, 8582.
3	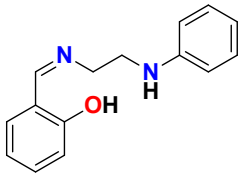	HEPES buffer (0.1 M) solution ($EtOH/H_2O$= 1 : 1 v/v, pH 7.4)	0.24 μM	Ghosha, A.; Das, D. *Dalton Trans.*, **2015**, *44*, 11797.
4	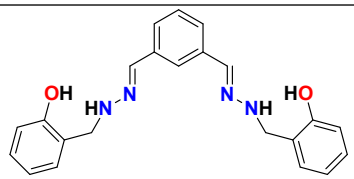	CH_3OH/H_2O	0.77 μM	Goswami, S.; Manna, A.; Paul, S.; Aich, K.; Dasa, A. K.; Chakrabortya, S. *Dalton Trans.*, **2013**, *42*, 8078.
5	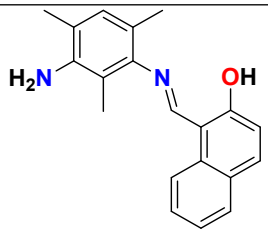	$MeCN/H_2O$ = 7:3 v/v, 10 μM HEPES buffer, pH = 7.4	0.086 μM	Saini, A. K.; Sharma, V.; Mathur, P.; Mobin, S. M. *Sci. Rep*. **2016**, *6*, 34807.
6	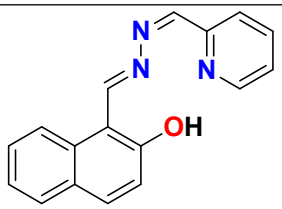	CH_3OH–aqueous HEPES buffer (5 mM, pH 7.3; 9 : 1, v/v)	2.8 μM	Samanta, S.; Goswami, S.; Hoque, M. N.; Ramesh, A.; Das, G. *Chem. Commun*., **2014**, *50*, 11833.
7	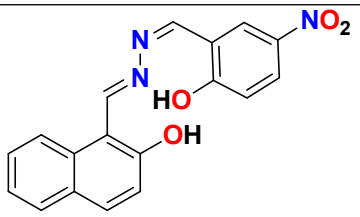	H_2O/CH_3OH	4.39 μM	Roy, A.; Dey, S.; Halder, S.; Roy, P. *J. Luminesc.* **2017**, *192*, 504.

8	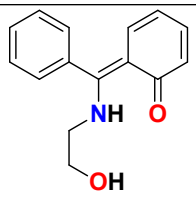	EtOH	0.1 μM	Naskar, B.; Modak, R.; Sikdar, Y.; Maiti, D. K.; Bauza, A.; Frontera, A.; Katarkar, A.; Chaudhuri, K.; Goswami, S. *Sensors Actuat. B, Chemical.*, **2017**, *16*, 1194.
9	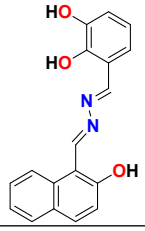	DMF/H_2O	0.042 μM	Saini, A. K.; Natarajan, K.; Mobin, S. M. *Chem. Commun.*, **2017**, *53*, 9870.

Table S3. Fluorescence lifetime parameters for **L4**, **L4** + $Al^{3+}$and **L4** + Ga^{3+}.

	τ_1 (ns)	τ_2 (ns)	B1	B2	τ_{av} (ns)
L4	0.907	4.171	0.135	0.041	2.82
L4 + Al^{3+}	0.961	4.258	0.097	0.062	3.40
L4 + Ga^{3+}	0.949	4.214	0.109	0.055	3.21